GEOLOGY AND GEOCHEMISTRY OF PALEOPROTEROZOIC MAGNESITE DEPOSITS (~1.8Ga), STATE OF CEARÁ, NORTHEASTERN BRAZIL

[1]Clóvis Vaz Parente, [2]Luis Henrique Ronchi, [3]Alcides Nóbrega Sial, [4]Jean Jacques Guillou, [1]Michel Henri Arthaud, [5]Kazuo Fuzikawa, and [1]César Ulisses Vieira Veríssimo

[1]Dept. of Geology, Federal Univer. of Ceará, Fortaleza, Ceará, 60.455-760 Brazil

[2]Dept. of Geology, Vale dos Sinos Univ, Rio Grande do Sul, Brazil

[3]NEG-LABISE, Dept. of Geology, Federal Univ. of Pernambuco, C.P. 7852, Recife, 50732-970, Brazil

[4]Laboratoire de Bio-geologie, 2 Boulevard Leverse, 49045, Angers Cedex 01, France

[5]Center of Development of Nuclear Technology, C.P. 941, Belo Horizonte, Minas Gerais, 30123-970, Brazil

ABSTRACT: Five important magnesite mines and small occurrences in the state of Ceará form a sequence of lenses that extend, discontinuously, for over 140km. The magnesite rocks are hosted by metadolomites with lutecite, sulphate nodules pseudomorphosed by fiber-radiated quartz, scapolite and dissolution breccias. This metacarbonate sequence is more voluminous and more calcic in the southwestern extremity of the belt, but less voluminous and more magnesian towards the northeastern portion of the belt, the highest Mg contents being observed in the Alencar-Orós region. Magnesite deposits pass gradually into metadolomites and then to almost pure calcitic marbles westward the belt. This group is hosted in a greenschists to amphibolite-facies metavolcanic-sedimentary sequence crosscut by basic sills and granitic intrusions of variable size, form, composition and age (middle to late Proterozoic ~550Ma).

Two types of magnesite marble may be distinguished: (1) medium-grained (1 to 9mm) and (2) sparry -magnesite marble (1 to 15cm). The latter displays wide textural variation (porphyric, rosette, layered and palisadic types) and exhibits remnants of the original sedimentary features. The sparry crystals, in spite of their deformation, are hypidiomorphic and pinolitic. The colors vary from white to light or dark gray, or even red. The dark banded term presents traces of microfossils and stromatolites structures. The medium-grained magnesite marble, on the other hand, shows more homogeneous texture and color and anhedral crystals are more abundant.

The sparry-magnesite marble is less enriched in SiO_2, Fe_2O_3, Al_2O_3 and CaO and richer in MgO than the medium-grained ones. The magnesitic marbles display positive Ce, and negative Eu anomalies. This suggests a shallow marine platform environment with continental, reduced influence (lagunar). These magnesitic marbles also show positive Ce and Eu anomalies in relation to the present seawater, suggesting compositional differences, materialized mainly by an enrichement of these elements in the past seawater.

Fluid inclusions in the medium-grained magnesites of the Riacho Fundo deposit are aqueous inclusions, while in the sparry magnesite deposits, particularly in Cabeça de Negro, aquo-carbonic inclusions dominate. Hydrocarbons, however, are found in both cases.

The calcitic marble, deposited on open-marine environment, displays positive ^{13}C (+0.5 to 2.1 ‰ PDB), while dolomitic to dolostone marbles, deposited on less open marine environment, display negative shift (0.7 to –3.2‰ PDB). This ^{13}C fluctuation is within the range for carbonates deposited around 1.8Ga.

The depositional environment of these carbonates is close to a paralic system, lagoon, with strong evaporitic conditions. The depressions were of variable depth and lengths and could be isolated, in particular by stromatolitic barriers, dried and flooded by seawater with continental inflows. The largest and deepest ones correspond to the sparry magnesite deposits. These magnesites are located in a lateral way to almost pure calcitic marbles, through dolomitic marbles. This points to a process of chemical differentiation within a paralic system, from open sea to landwards, more calcic in the first to more magnesian in the confined environment, in which lagoon waters are progressively purified from Ca through preferential precipitation of calcic carbonates and secondly of gypsum/anhydrite, which increases the Mg/Ca ratio, and lead carbonate deposits towards the magnesite pole. These metacarbonates also reveal a fractionation of the light REE, starting from the calcitic, through the dolomitic to magnesitic marbles. In the calcitic marbles, REE are in association with the clay fraction, while in magnesitic marbles, they seem to be in association with organic and/or soluble complexes. The magnesitic marbles are of sedimentary origin and underwent important diagenetic evolution before being metamorphosed during the Brasiliano orogenic cycle.

INTRODUCTION

Magnesite, as an accessory phase or forming small bodies without economic importance, may be found in a series of geological environments, from the Archean to the Cenozoic. At present, magnesite is associated with lacustrine deposits of arid climate (Elton lake, ex. URSS; Tuz Gölu, Turkey) and with saline to hypersaline paralic deposits (Coorong, Australia; sabkha El Melah, Tunisia; sabkhas of the Pirate coast, Arabic Gulf) (Müller et al. 1972; Von der Borg 1965; Busson and Perthuisot 1977). It is also asociated with calcretes (Australia), with laterites developed on ultrabasic rocks, with contact metamorphic zones and with hydrothermal veins.

The largest magnesite deposits are, however, hosted by Proterozoic and Paleozoic terrains associated to rocks of sedimentary origin, known as of Veitsch type (Pohl and Siegl 1986; Pohl 1989). The origin of the magnesite deposits of this type, however, is controversial and two hypotheses are known (1) syngenetic formation; (2) epigenetic formation or metasomatic.

A genetic model that assumes magnesite to be syn-

sedimentary or formed during early diagenesis, if dolomite is a primary precipitated phase, is based on recent sedimentary systems (e.g., Rumpf 1873 in Pohl and Siegl 1986; Nishihara 1956; Gomes de Llarena 1968; Valdiya 1968; Quéméneur 1974; Guillou 1973, 1980; Chaye d'Albissin and Guillou 1986, 1988; Pohl and Siegl 1986; Pohl 1990; Velasco et al. 1987; Guillou and Letolle 1988; Qiusheng 1988; Almeida 1989; Tufar et al. 1989, Joshi et al. 1993, Melezhik et al. 1997, Melezhik et al. 2001).

A metasomatic hypothesis in which magnesite results from the introduction of ions of Mg^{2+} during metamorphism of limestones or dolomite precursors, has been proposed by several authors (e.g., Koch 1893 in Pohl and Siegl 1986; Bodenlos 1948, 1954; Morteani et al. 1982, 1983; Bone 1983; Aharon 1988; Morteani 1989; Kralik et al. 1989; Möller 1989; Preinfalk et al. 1993; Lugli et al. 2000).

Hypotheses on the origin of magnesite associated to metasedimentary rocks are, therefore, numerous and, in general, based on particular characteristics of the studied deposits, normally envolving one single type of occurrence of magnesite.

There are two important types of precambrian magnesite deposits in the state of Ceará. They are 40km apart, but they are related to the same lithostratigraphic unit: (a) fine- to medium-grained and (b) coarse-grained or sparry magnesite deposits.

The present study, based on fluid inclusions, elemental and isotope geochemistry of magnesite deposits of the Ceará state, offers an opportunity to advance with the knowledge of the geology and genesis of precambrian magnesite deposits associated with metasedimentary rocks.

GEOLOGIC FRAMEWORK OF THE OROS FOLD BELT

The Orós foldbelt is part of the set of proterozoic foldbelts that comprises the Borborema province, constituted by supracrustal rocks of the late Paleoproterozoic within archean or early paleoproterozoic rocks of the basement. The Orós foldbelt forms a sigmoidal, linear zone whose structural trends vary from ENE-WSW in its western portion, to N-S in the central one, and to NE-SW in its northern extremity. The belt extends for over 600 km with a width that varies from 2 to 13km.

The basement is composed of meso- to leucocratic orthogneiss of tonalitic to trondjemitic composition, partially migmatized, with equigranular to pegmatitic granodioritic mobilizates bordered by biotitic fringes. Partially migmatized paragneisses with quartz-feldspathic mobilizates and biotitic fringes (melanosome), biotite restites, two-mica peraluminous granites, garnet-sillimanite schists and garnet-bearing calc-silicate rocks are also observed. Orthogneisses from the basement are about 2.1Ga old (U-Pb in zircon; Landim 2000).

The supracrustal sequence is dominated by metasedimentary rocks and basic to acidic metavolcanics. The metasedimentary rocks are represented by schists and aluminous quartzites discontinuously covered by marine carbonates and evaporites, represented by calcitic, dolomitic and magnesitic marbles and calc-silicate rocks. The schists comprise andalusite-rich schists, garnet-staurolite-andalusite schists, two-mica garnet-schists, and feldspathic schists or metagreywackes. The andalusite-rich schists and the garnet-staurolite-andalusite schists are found in the eastern portion near the base of the sequence, while the other lithological types are located in the upper portion of the system.

Quartzites are usually in topographic relief and intercalated in schists as discontinuous, tens of meter thick, few kilometers long bodies (e.g. Orós and Franco hills) and as small, cross-stratified, few meter thick, lenticular bodies within the metapelitic sequence. They are very abundant in the northeastern portion of the belt and, progressively, decrease in volume and extension towards the southwestern extremity of the belt. The carbonate sequence, on the contrary, is more abundant and more calcic in the southeastern extremity of the belt (Pio IX and Aiuaba regions), becoming more magnesian and decreasing in volume and extension, in the northeastern portion of the belt (e.g. Alencar-Orós region). These are features common to a mixed paralic-deltaic system.

The metavolcanic-sedimentary sequence was deformed and metamorphosed under greenschist to amphibolite facies with narrow isoclinal folds, with vertical axial plane foliation and subhorizontal stretching lineations consistent with a Brasiliano transpressional regime. Further details on the geology of this area are found in Sá (1991), Parente (1995) and Parente and Arthaud (1995).

GEOLOGY OF THE MAGNESITE DEPOSITS

The main deposits and some magnesite occurrences in the state of Ceará form a string of lenses that integrates a discontinuous carbonate rock set, 140km long, between Pio IX in the state of Piaui, to the west and Orós, Ceara state to the east (Fig. 1). All of these metacarbonate rocks are interlayered in the greenschist to amphibolite facies metavolcanic-sedimentary sequence intruded by mesoproterozoic and neopaleozoic granites and by neoproterozoic basic-ultrabasic plutons.

Thermobarometric studies on aluminous schists (Sá 1991) with or without staurolite, in contact with sparry magnesite marbles, yielded temperature values, respectively, between 443 and 507°C and 436 and 485°C, and pressure P around 3kbar. U-Pb dating for some rhyolites intercalated with

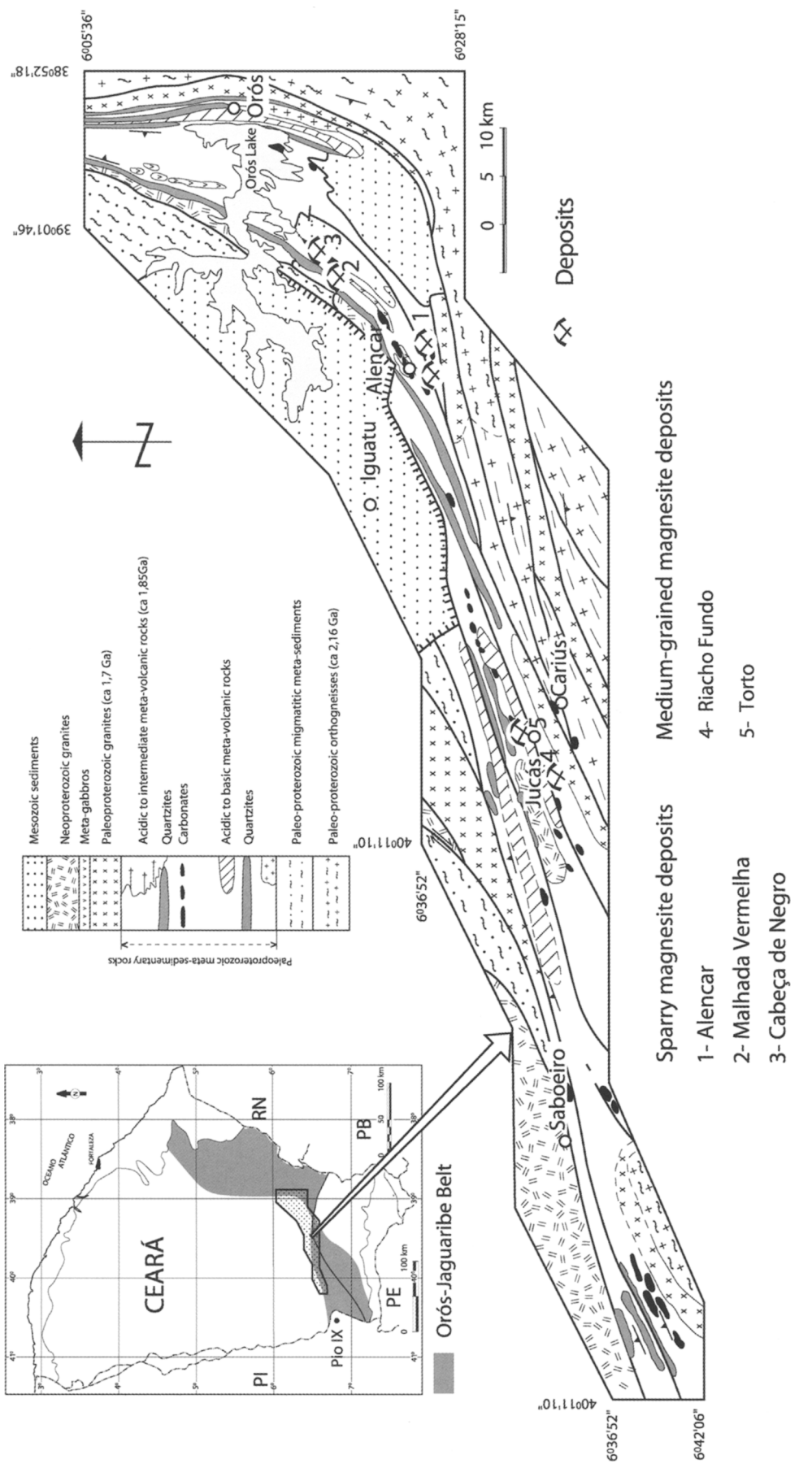

Figure 1. Geological map of the Oros Belt (modified from Sa' 1991 and Parente 1995).

metasedimentary rocks revealed ages around 1.8Ga (Sá 1991; Van Schmus et al. 1995; Landim 2000), corresponding to the sedimentation age.

Two types of magnesitic marbles have been distinguished: (a) sparry magnesitic (1 to 15cm long magnesite crystals) and (b) medium-grained magnesitic marbles (1 to 9mm crystals).

CHARACTERISTICS OF THE SPARRY MAGNESITE DEPOSITS

The sparry magnesite deposits (Alencar, Malhada Vermelha and Cabeça Negro) and some occurrences are located in the central-eastern portion of the belt between Alencar and Orós. They form a 25km-long string of discontinuous lenticular bodies. The length of these lenticular bodies vary from 20 to 900m long and the width, from 10 to 200m. The largest deposits are found in the Alencar region, but those with best preserved primary structures are in the Cabeça de Negro region.

The magnesites are found in association with dolomitic marbles, where one verifies locally the development of lutecite, scapolite, sulfate nodules pseudomorphically replaced by fiber-radiated quartz crystals, dissolution breccias and dolomitic marbles with petal-shaped texture. All of this association indicates that evaporitic conditions prevailed in the wall rocks of the magnesites. Further details on the formation of evaporitic older associations are found in Shaw (1960), Hietanen (1967), Serdyuchenko (1975), Badham and Stanworth (1977), Hogarth and Griffin (1978), Leake and Farrow (1979), Arbey (1980), Friedman (1980), Friedman and Shukla (1980), Vanko and Bischop (1982), Papaioanou and Carotsieris (1993), Svenningsen (1994) and Parente et al. (1996).

The transition of sparry magnesitic marbles into dolomitic marbles is gradual and well-defined but, sometimes, complex when a mixture between these carbonate rocks occur. This suggests in situ mixture between these two lithological types or an incomplete replacement of one by the other. Sparry magnesitic veins are seen crosscutting metadolomites.

The sparry magnesitic marbles exhibit textural variations where porphyritic, rosette, banded or palisade varieties are common. The last one preserves some of the original sedimentary structures. Traces of microfossils are found with the banded textures, while stromatolitic structures are found with the other textural varieties. The color of these rocks vary from white, to light to dark gray, pink to brick-red. Crystals are usually subidiomorphic to subautomorphic and their size varies from 1 to 15 cm.

Some magnesitites show up to 21% SiO_2 and have talc and chlorite while others are Fe-enriched and show iron oxide minerals and syn-metamorphic pyrite which appears in veins or as nodules.

The two small lenticular deposits of the Alencar region (Fig. 2) exhibit stromatolitic relicts and microfossils, besides irregular pyrite veins, with nodular texture. They also exhibit silica-enriched layers with chlorite and talc or some iron-enriched ones. This observation leads to the assumption that these deposits may represent a marginal lagunar zone with periodic inflow of continental water containing silica and probably iron. The stromatolitic facies corresponds either to stromatolite barriers in the lagunar entrance or to intralagunar formations.

The Malhada Vermelha deposit (Fig. 3) is also characterized by iron oxide and silica enrichment. In this deposit, the transition between the magnesites and the dolomitic marbles is marked by a thin layer of metadolomite (1m thick) with quartz nodules in a ferruginous and brecciated

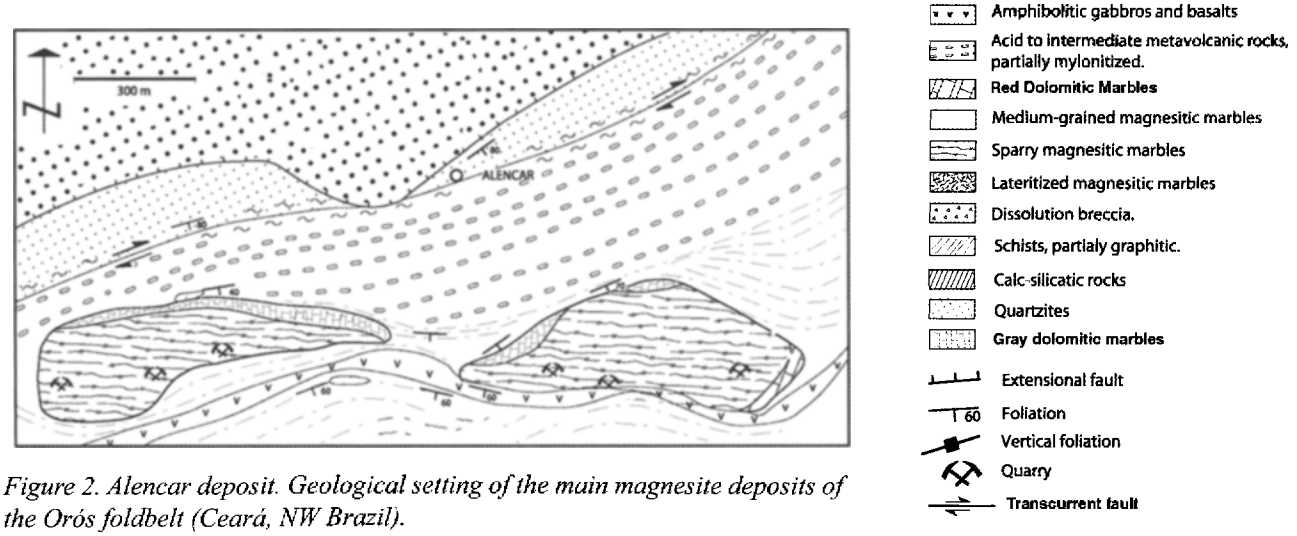

Figure 2. Alencar deposit. Geological setting of the main magnesite deposits of the Orós foldbelt (Ceará, NW Brazil).

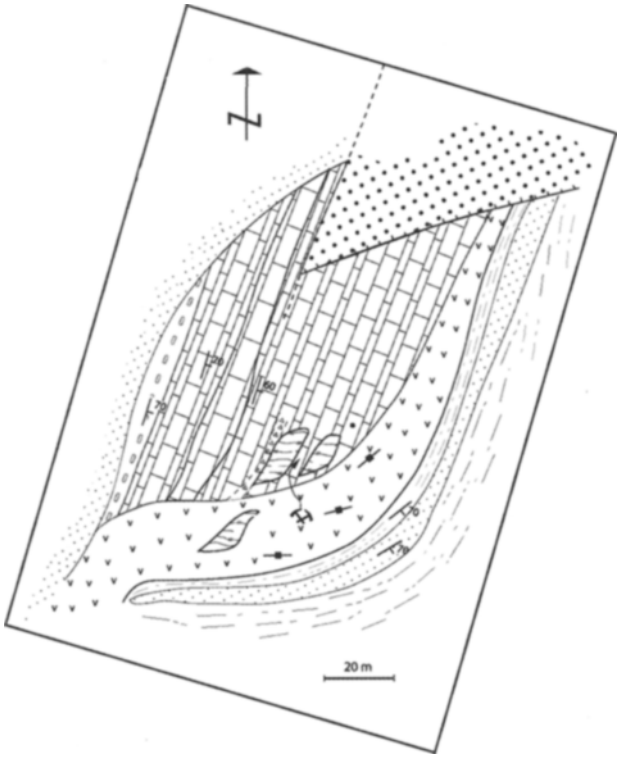

Figure 3. Malhada Vermelha deposit. Geological setting of the main magnesite deposits of the Orós foldbelt (Ceará, NW Brazil).

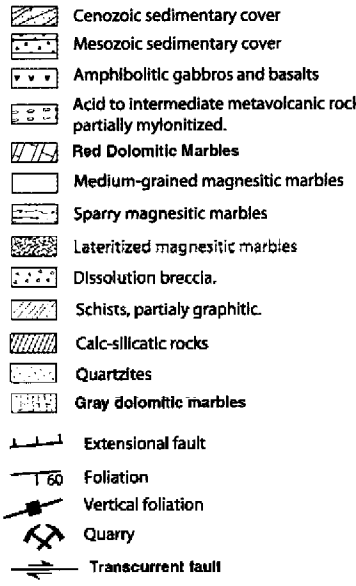

dolomitic matrix. These nodules are ellipsoidal, with major axis between 1 and 10cm. They are constituted by fiber-radiated quartz as rosettes, indicating they are sulphate pseudomorphs replaced by silica. There are also even more brecciated metadolomites, typical of dissolution breccias found in evaporite deposits. In these breccias, one finds lutecite crystals with dolomite inclusions, some of them automorphic and cubic, indicating they are halite pseudomorphs replaced by dolomite.

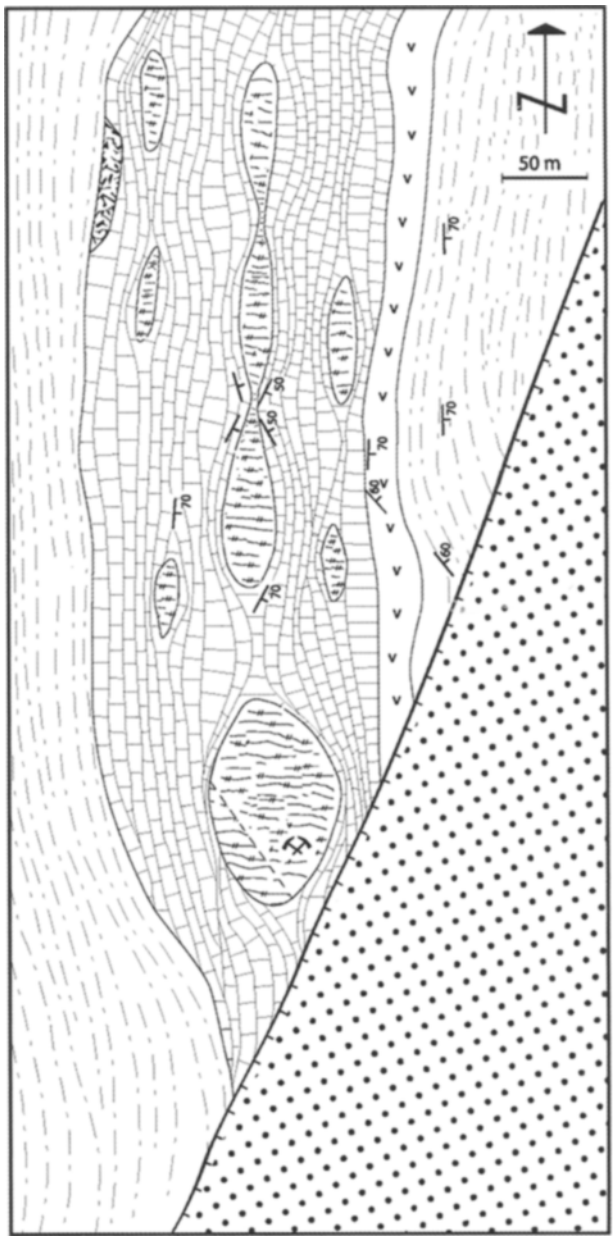

Figure 4. Cabeça de Negro deposit. Geological setting of the main magnesite deposits of the Orós foldbelt (Ceará, NW Brazil).

These breccias appear to record a temporal-spatial hiatus between the dolomitic and the magnesitic carbonates. One can interpret this as an indication of a late accumulation of continental sabkhas in the contact zone, accompanied by dissolution and/or redistribution of the evaporites.

The Cabeça de Negro deposit shows boudinated mega- and micro-structures, where the magnesites, enclosed by metadolomites with scapolite, correspond to the more competent terms or less deformed ones in this set (Fig. 4). Magnesitic marbles exhibit, in general, palisade texture marked by alternance of magnesite crystals with

dark millimetric zones, enriched in pelitic and/or organic material. The magnesite crystals are of the pinolitic type, sub-automorphic and with an average size of 1cm, exhibit a bi-polar growth in symmetry to pelitic and/or organogenic levels (Fig. 5a). These crystals are deformed, curved and, under the microscope, are marked by wavy extinction, deformation bands and recrystallization into subgrains, and this indicates that they are pretectonic crystals. The color of these rocks varies from white, light to dark gray, to pink to brick-red.

The predominance of small lenticular magnesitite with palisade structures/textures with metadolomites, appear to reflect rhythmic variation in the middle of the carbonate sedimentation. These variations can be associated with, among other phenomena, oscillations of the sea level. Besides these features, there are also Al-silicate and Fe-enriched magnesite and metadolomite levels with detrital zircon which could indicate freshwater inflow during the formation of this deposit.

All of these features indicate that sparry magnesitic marbles formed in paralic systems, lagunar with marked evaporitic tendency, receiving periodical inflow of freshwater.

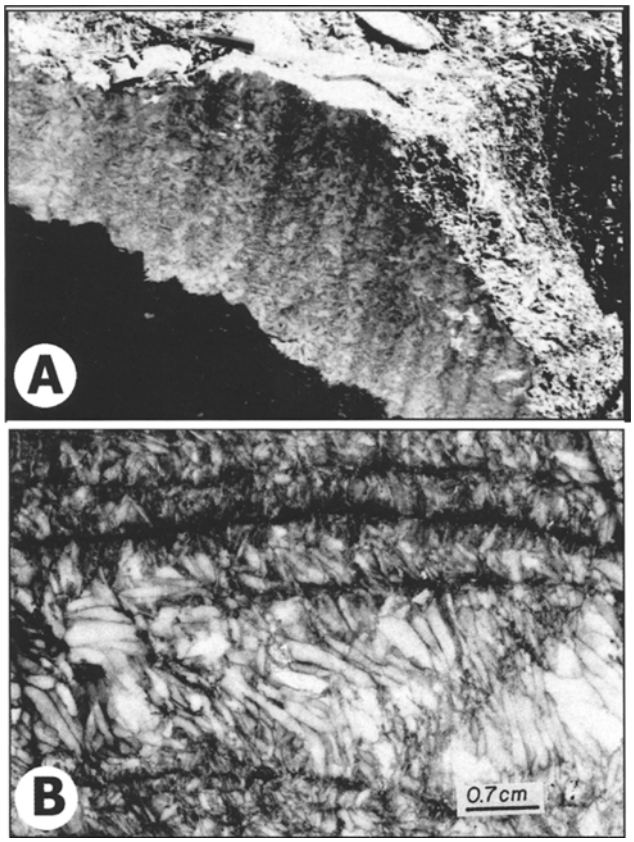

Figure 5. (A) Outcrop of sparry magnestitic marble with palisade structure. S0 // S1 stratification marked by thin layers of organic matter or dark gray pelite in alternance with light gray sparry magnesite. Cabeça de Negro deposit. Notice the hammer at the left upper side. (B) Sparry magnesitic marbles with deformed palisade structure. Bent magnesite crystals apparently indicate left-lateral movement.

CHARACTERISTICS OF MEDIUM-GRAINED MAGNESITE DEPOSITS

The medium-grained magnesitic deposits are represented by small lenticular bodies in the central-western portion of the belt (Jucás region), known as Riacho Fundo and

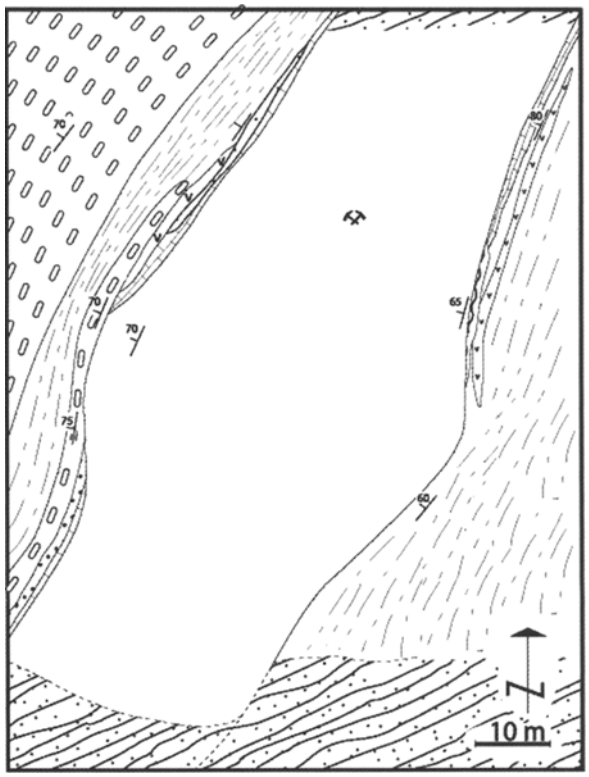

Figure 6. Riacho Fundo deposit. Geological setting of the main magnesite deposits of the Orós foldbelt (Ceará, NW Brazil).

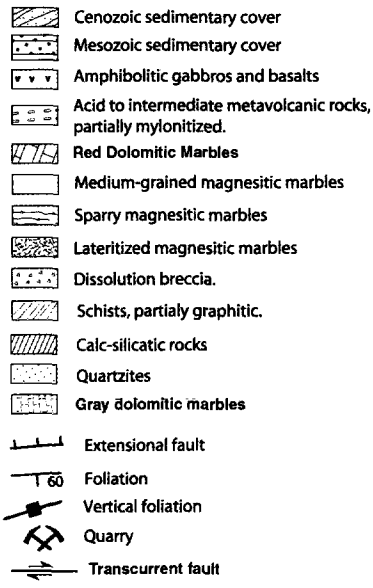

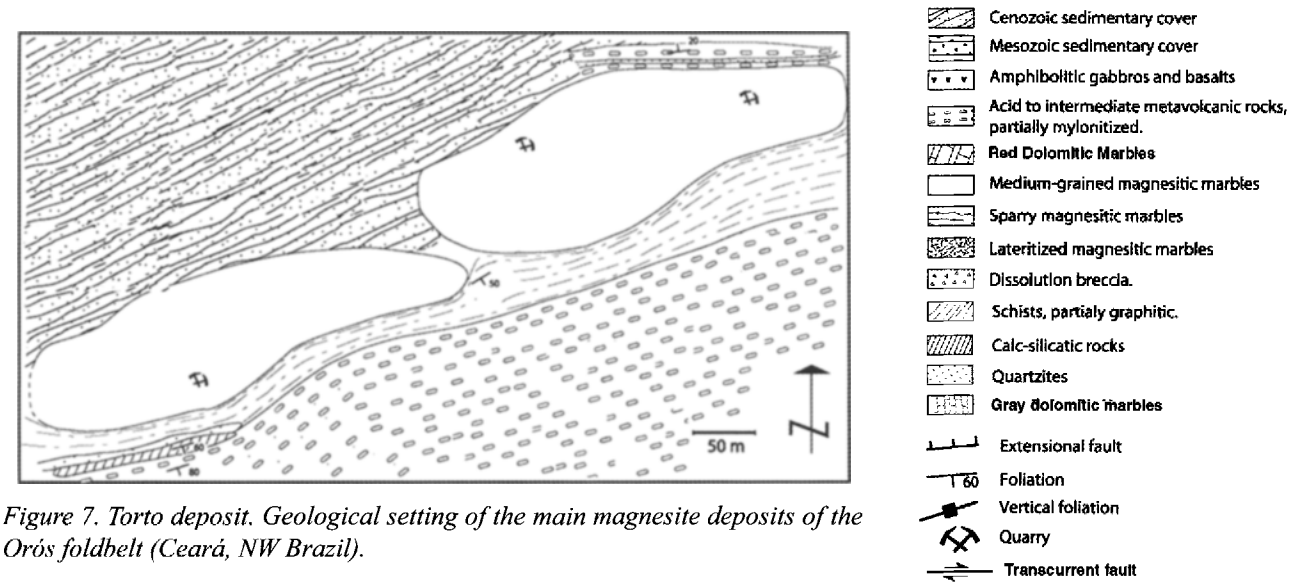

Figure 7. Torto deposit. Geological setting of the main magnesite deposits of the Orós foldbelt (Ceará, NW Brazil).

Torto (Figs. 6 and 7). They occupy two small basins, presently separated by a structural accident, which preclude comparing them stratigraphically: the metavolcanic acidic rocks and Jucás porphyritic metagranites represent the central portion of this structural accident. The Riacho Fundo magnesite deposits display a lenticular shape and irregular thickness, due to a pinch-and-swell megastructure, partially controlled by ductile shear zones. This well-exploited deposit is about 100m long and about 30 to 50m thick, and its extremities are covered by cenozoic sediments. It is intercalated in light gray metadolomites, in basic schists with biotite, phlogopite and tremolite and in scapolite-bearing calc-silicate rocks.

From the petrographic viewpoint, the magnesitic marbles are very homogeneous and characterized by a fine to medium-grained dominant facies (1 to 8mm), white color, sometimes with light to dark gray patches. Locally, some textural/structural variations are observed, and subrounded magnesite grains, 3 to 6mm in diameter, are seen in a matrix with talc and chlorite (Fig. 8a) or in veins filling extensional fractures opened during deformation. In this case, the magnesitic marble is characterized by 1 cm-long, translucid, prismatic magnesite crystals, developed perpendicular to the walls of the talc-choritic levels.

Under the microscope, the fine- to medium-grained facies is characterized by an allotriomorphic, granoblastic texture essentially composed by magnesite, with talc, chlorite and pyrite accessory phases. The largest magnesite crystals, up to 8mm long, are marked by sutured boundaries, wavy extinctions, deformational bands and recrystallization and are usually clouded with small dark inclusions (organic matter?), oriented or not. Small magnesite grains, usually pure, display straight boundaries or slightly bent and triple junctions and are product of recrystallization. Subrounded magnesite, sometimes sigmoidal, when deformed displays a pyrite-, talc- and chlorite-rich nucleus, besides fluid inclusions disposed in radial lines (Fig. 8b). This spheroidal texture, only seen in this deposit suggests three possibilities: (a) replacement of oolitic structures or pre-existing carbonate oolites (radial magnesian calcite);

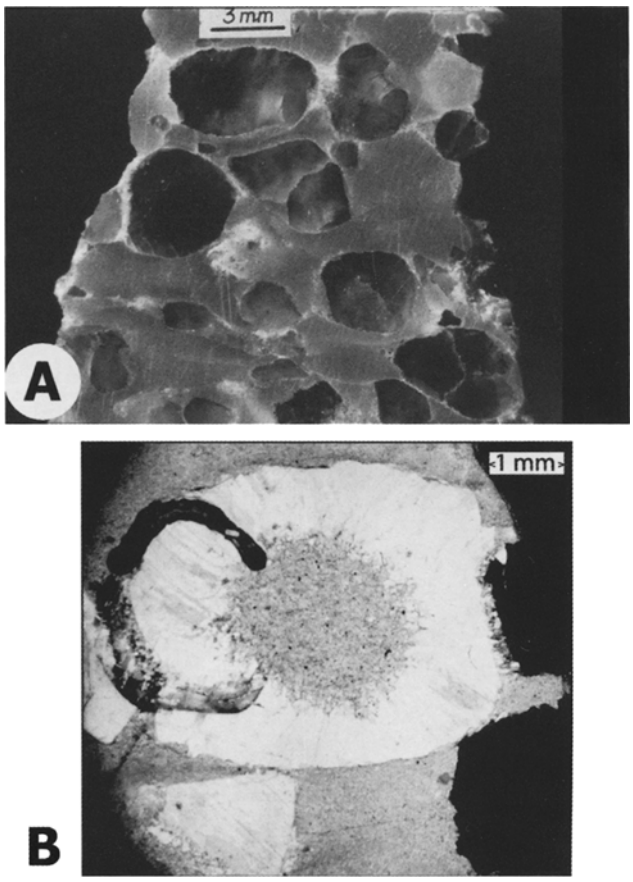

Figure 8. (A) Ovoid crystals of magnesite deformed to a sigmoidal form, in a talc and ferromagnesian-rich matrix. (B) Magnesite crystals with pyrite micro-inclusions in its nucleus (opaque crystals), of sedimentary origin, suggesting organic matter-rich micro-environments (sulfate-reducing bacteria) in hypersaline environments.

Table 1. Chemical analyses of major elements (%) of meta carbonatic rocks from the Orós foldbelt.

	Calcitic marble						Dolomitic marble						
	CMMD 1M	CMMD 1N	CMMD 1P	CMMD 5A	CMMD 5B	X	CMMD 6C	CMMD 6D	CMMD 7F	CMMD 8I	CMMD 8J	CMMD 8L	X
%													
CaO	49.8	54	54.1	47.4	52.8	51.62	25.7	29.9	29.8	27.4	28.9	28.6	28.38
MgO	3	1.5	0.65	4.6	1.7	2.29	21.4	21..8	21.8	23.1	22.5	21.4	22
Al_2O_3	0.69	0.12	0.18	1.1	0.45	0.51	1.1	0.51	0.1	1.1	0.21	0.22	0.54
Fe_2O_3	0.45	0.1	0.01	0.1	0.13	0.16	0.94	0.28	0.2	0.1	0.1	0.21	0.31
FeO	0.14	0.14	0.28	0.28	0.14	0.2	0.28	0.28	0.14	0.28	0.28	0.14	0.23
SiO2	5.7	0.79	1.6	4.5	1.5	2.82	10.6	0.92	1.5	3.9	3.2	4.8	4.15
MnO	0.01	0.01	0.02	0.01	0.01	0.01	0.07	0.06	0.04	0.02	0.02	0.02	0.04
P_2O_5	0.05	0.05	0.05	0.05	0.06	0.05	0.05	0.05	0.05	0.05	0.05	0.05	0.05
TiO_2	0.05	0.05	0.05	0.06	0.05	0.05	0.06	0.05	0.05	0.08	0.05	0.05	0.06

	Dolomitic calcitic marble				Magnesitic marble								
	CMMD 6A	CMMD 6B	CMMD 6F	X	CMMD 7C	CMMD 7D	CMMD 7E	CMMD 8A	CMMD 8B	CMMD 8C	CMMD 8D	CMMD 8H	X
%													
CaO	35	46.9	48.3	43.4	0.73	0.6	8.4	0.41	1.7	1.7	1.1	1	2.06
MgO	14.6	6.9	5.7	9.07	46.4	46.1	39.2	46.6	45.4	44.9	44	44.7	44.66
Al_2O_3	1.5	0.06	0.11	0.56	0.15	0.28	0.31	0.11	0.26	0.36	1.3	0.4	0.4
Fe_2O_3	1.2	0.33	0.53	0.69	0.4	0.36	0.7	0.42	0.36	0.14	0.46	0.98	0.48
FeO	0.42	0.42	0.14	0.33	0.28	0.28	0.42	0.42	0.42	0.56	0.42	0.14	0.37
SiO_2	5.2	1.8	1.4	2.8	1.2	3.1	2.1	0.47	2.4	3.3	7.1	2.5	2.77
MnO	0.23	0.37	0.29	0.3	0.03	0.03	0.08	0.06	0.04	0.03	0.04	0.06	0.05
P_2O_5	0.11	0.05	0.05	0.07	0.05	0.05	0.05	0.05	0.05	0.05	0.05	0.05	0.05
TiO_2	0.18	0.05	0.05	0.09	0.05	0.05	0.05	0.05	0.05	0.05	0.07	0.05	0.05

(b) pseudomorphs of crystals percursors of magnesite, like nesquehonite or huntite; (c) the original shape of magnesite.

The Torto mine is characterized by two small lenses, roughly sigmoidal, with up to 400m long and up to 120m wide, trending NE-SW, and dipping subvertically. The transition between these two lenticular bodies is covered by clayey soil. These lenticular bodies are boundered to the south by metadolomites, pyrite-rich graphite-schists, quartzites, calc-silicate rocks and porphyritic metadacite while, to the north, one finds thin films of metarhyolites and mylonitized quartzites. From the petrographic viewpoint, two facies are identified: a fine-grained facies (1-2mm) located in the center of the quarry and a very deformed, equigranular, medium-grained (3-5mm) in the southern portion of the southern lenticular body. Both are dominated by magnesite; talc and chlorite are secondary minerals as well as dolomite in veins that filled one-cm wide fractures.

MAJOR, TRACE AND RARE EARTH ELEMENT GEOCHEMISTRY

A total of twenty two carbonate samples in this study were analyzed in the GEOSOL Laboratories (GEOLAB), in Belo Horizonte. SiO_2, Al_2O_3, total FeO, CaO, MgO, MnO, P_2O_5 and TiO_2 have been determined by X-ray fluorescence in samples fused with $Li_2B_4O_7$. FeO was analyzed after reaction with HF + H_2SO_4 in a platinum crucible, release of CO_2 and titration of FeO with $KMnO_4$ and boric acid. Rare-earth elements were analyzed in an ARL ICP 3500.

Among these samples, 5 are from calcitic marbles of the western zone of the belt, between Cruzeta (Ceará) and Pio IX (Piaui); 9 samples are from dolomitic marbles, that are wall rocks of the sparry magnesites, in the central-eastern portion of the belt, next to the Malhada Vermelha and Cabeça de Negro deposits, and 8 are from sparry magnesites from the Cabeça de Negro deposit. Among the dolomitic marble samples, 3 are of brecciated dolomitic marbles, cemented by sparry calcite (Tables 1 and 2).

Major Element Behavior

Major elements in the metacarbonates under consideration have been plotted in the Fe_2O_3+FeO-CaO – MgO (Fig. 9a) and Fe_2O_3+FeO+SiO_2-CaO – MgO (Fig. 9b) diagrams. These rocks plot preferentially in the magnesitic, dolomitic and calcitic marble fields.

Table 2. Rare-earth element concentration (ppm) in metacarbonate rocks of the Orós foldbelt.

	Sample	La	Ce	Nd	Sm	Eu	Gd	Dy	Ho	Er	Yb	Lu	Total	La/Lun	Eu/Eun
Calcitic marble	CMD1M	4.098	7.887	2.364	0.370	0.047	0.198	0.169	0.036	0.092	0.072	0.009	14.349	47.265	0.481
""	CMD1N	1.947	3.486	1.017	0.157	0.024	0.100	0.057	0.012	0.038	0.023	0.004	6.450	50.526	0.548
""	CMD1P	2.940	5.239	1.480	0.249	0.068	0.190	0.128	0.023	0.047	0.039	0.005	9.659	61.036	0.920
""	CMD5A	5.683	13.480	4.310	0.750	0.145	0.626	0.407	0.080	0.200	0.157	0.028	23.473	21.068	0.630
""	CMD5B	3.344	7.154	2.373	0.417	0.058	0.239	0.191	0.041	0.095	0.072	0.010	12.871	34.711	0.516
Dolomitic calcitic marble	CMD6A	12.560	57.450	22.710	5.637	1.042	4.248	4.557	0.899	2.352	1.920	0.280	112.476	4.656	0.626
""	CMD6B	8.548	18.560	5.223	0.918	0.202	0.660	0.483	0.095	0.230	0.180	0.031	32.331	28.623	0.758
""	CMD6F	5.984	16.420	6.810	1.060	0.188	0.661	0.458	0.080	0.220	0.160	0.026	30.274	23.890	0.640
Dolomitic marble	CMD6C	4.886	11.340	4.400	0.780	0.116	0.434	0.302	0.054	0.151	0.148	0.027	20.626	18.784	0.556
""	CMD6D	4.573	10.470	3.850	0.700	0.120	0.363	0.320	0.072	0.160	0.133	0.027	18.893	17.581	0.654
""	CMD7F	3.729	9.348	3.138	0.600	0.159	0.444	0.310	0.063	0.155	0.102	0.018	16.215	21.504	0.903
""	CMD8I	3.773	10.050	5.180	0.940	0.169	0.746	0.508	0.110	0.250	0.228	0.037	19.003	10.585	0.597
""	CMD8J	2.617	6.615	2.155	0.350	0.096	0.295	0.231	0.046	0.110	0.123	0.020	11.387	13.583	0.890
""	CMD8L	3.568	8.362	3.510	0.680	0.105	0.463	0.360	0.080	0.220	0.176	0.037	15.440	10.010	0.542
Magnesi-tic marble	CMD7C	2.188	6.238	3.137	0.680	0.136	0.625	0.530	0.097	0.250	0.216	0.036	11.563	6.309	0.627
""	CMD7D	1.405	4.389	2.442	0.550	0.113	0.484	0.410	0.087	0.230	0.184	0.029	8.236	5.029	0.656
""	CMD7E	1.133	2.872	1.322	0.268	0.058	0.158	0.100	0.018	0.045	0.039	0.006	5.327	19.601	0.795
""	CMD8A	1.234	3.967	1.874	0.370	0.085	0.366	0.240	0.063	0.160	0.131	0.029	7.075	4.417	0.699
""	CMD8B	1.718	5.386	2.644	0.680	0.140	0.645	0.530	0.112	0.270	0.240	0.045	9.748	3.963	0.637
""	CMD8C	1.481	4.554	2.531	0.610	0.141	0.613	0.630	0.100	0.261	0.227	0.037	8.566	4.155	0.698
""	CMD8D	1.485	5.017	2.602	0.550	0.091	0.503	0.410	0.080	0.230	0.234	0.037	9.104	4.166	0.520
""	CMD8H	1.512	5.107	2.660	0.600	0.114	0.571	0.470	0.100	0.261	0.220	0.037	9.279	4.242	0.587

In the sparry magnesitic marbles, MgO varies from 39.20 to 46.60% with the lowest contents in the transition zones to the metadolomites. In turn, CaO varies from 0.41 to 8.40% with the highest values in the contacts with the dolomitic marbles. SiO_2 varies from 0.47 to 7.10 %; Al_2O_3 from 0.11 to 1.30% and Fe_2O_3 values are lower than 1% (0.14 to 0.98%). MnO varies from 0.03 to 0.08% with highest values found next to the dolomitic marbles. P_2O_5 presents low contents and usually around 0.05% while TiO_2 varies from 0.05 to 0.07%.

Dolomitic marbles exhibit MgO from 5.70 to 23.10% (avg. 17.69%) the lowest values found in calciferous dolomitic marbles. SiO_2 varies from 0.92 to 10.60% (avg. 3.70%); Al_2O_3 ranges from 0.06 to 1.50% (avg. 0.55%) and total FeO lower than 2% (0.24 to 1.62). CaO varies from 25.70 to 48.30% (avg. 33.39%) and MnO, from 0.02 to 0.37% (avg. 0.12%) much higher than values found in the associated to the sparry magnesites. The P_2O_5 varies from 0.05 to 0.11% (avg. 0.06) and TiO_2 range from 0.05 to 0.18% (avg. 0.07%).

The calcitic marbles located to the west of the belt display CaO from 47.40 to 54.10%. The lowest contents are in the samples next to the dolomitic marbles. SiO_2 is relatively low, varying from 0.79 to 5.70%, typical of plataformal limestone (e.g.Veizer et al. 1990); Al_2O_3 varies from 0.12 to 1.10% and total FeO is lower to 1% (0.15 to 0. 73%). MgO values are progressively higher from west to east and ranges from 0.65 to 4.60 %. MnO ranges from 0.01 to 0.02% whereas P_2O_5 and TiO_2 display average values around 0.05%.

In the magnesitic marbles, SiO_2 displays a strong positive

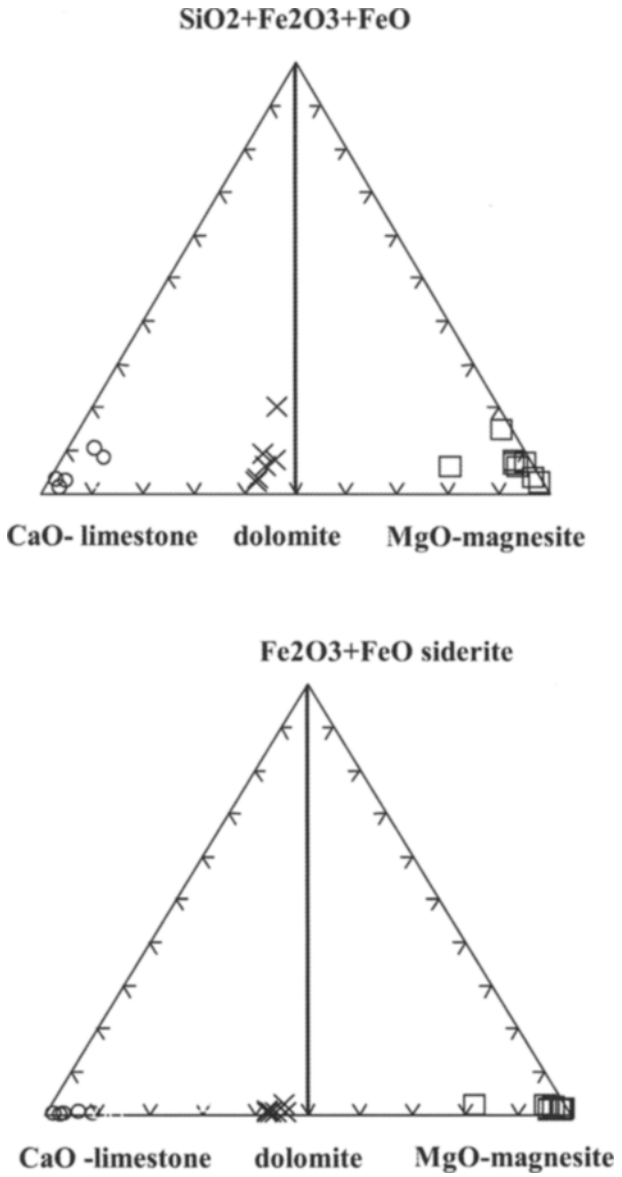

Figure 9. (A) Total Fe-CaO-MgO and (b) Total Fe-SiO_2-CaO-MgO diagram for metacarbonate rocks Alencar-Pio IX region. Open circles - calcitic marble from Pio IX and west of Cruzeta; cross: dolomite from Malhada Vermelha and Cabeça de Negro; triangle: calcic dolomite from Malhada Vermelha; square: sparry magnesite from Cabeça de Negro.

correlation with Al_2O_3 (r = 0.95; Table 3) and weak negative correlation with Fe_2O_3, MgO and MnO (r < -0.5). Fe_2O_3 and MnO vary sympathetically and both, along with CaO, show a negative correlation with MgO. A good correlation between SiO_2 and Al_2O_3 indicate that SiO_2 appears in magnesite associated with Al-silicate minerals and not as free SiO_2. The weak correlation, positive or negative, between Fe_2O_3 and Al_2O_3 and between Fe_2O_3 and SiO_2 demonstrate that the Al-silicate minerals correspond to Fe-poor chlorite (clinochlore) or to illite, as depicted from Fig. 10a. Other oxides like P_2O_5 and TiOs do not display co-variation with MgO as shown by a low correlation factor (r < 0.3, Table 3).

In the dolomitic marbles, SiO_2 shows positive correlation with Al_2O_3, Fe_2O_3 and MgO and negative with MnO, although with a correlation factor (r) lower than that for magnesites (Table 4). Fe_2O_3 varies sympathetically with MnO and both with CaO present a negative correlation with MgO. The low positive correlation between SiO_2 and Al_2O_3, Fe_2O_3 and Al_2O_3 and Fe_2O_3 with SiO_2 demonstrate that, in the dolomites, silica may be found as a free phase (quartz) or as an Al-silicate mineral mineral. As to the Al-silicate phase, this corresponds to a chlorite more Fe-enriched than that associated to sparry magnesites or to illite (Fig. 10a). P_2O_5 and TiO_2 do not exhibit co-variation with MgO (r<0.2).

In the calcitic marbles, SiO_2 display positive correlation with Al_2O_3, Fe_2O_3 and MgO (Table 5). Fe_2O_3 presents a negative correlation with MnO, as well as CaO vs. MgO. The positive correlation between Fe_2O_3 with Al_2O_3 and Fe_2O_3 with SiO_2 suggests that the Al-silicate phase associated with the limestones corresponds to a chlorite, more Fe-enriched, or to an illite, as one can see in Fig. 10a. P_2O_5 and TiO_2 shows very low correlation with MgO (r< 0.3).

The transition between the calcitic to magnesitic marbles is attained through dolomitic marble, marked by a sharp decrease of Ca from the calcitic into the sparry magnesitic marbles (Fig. 10b). Parente (1995) also observed a decrease from silica and alumina from metadolomites towards magnesitites. The decrease of silica and alumina in a carbonate sequence may reflect a chemical differentiation

Table 3. Correlation matrix for magnesitic marbles.

	CaO	MgO	Al_2O_3	Fe_2O_3	FeO	SiO_2	MnO	P_2O_5	TiO_2
TiO_2	-0.15	-0.11	0.97	-0.03	0.17	0.88	-0.14	0	
P_2O_5	0	0	0	0	0	0	0		
MnO	0.73	-0.69	-0.1	0.7	-0.09	-0.28			
SiO_2	-0.08	-0.18	0.95	-0.08	0.18				
FeO	0.17	-0.2	0.13	-0.7					
Fe_2O_3	0.39	-0.42	0.07						
Al_2O_3	-0.06	-0.22							
MgO	-0.96								

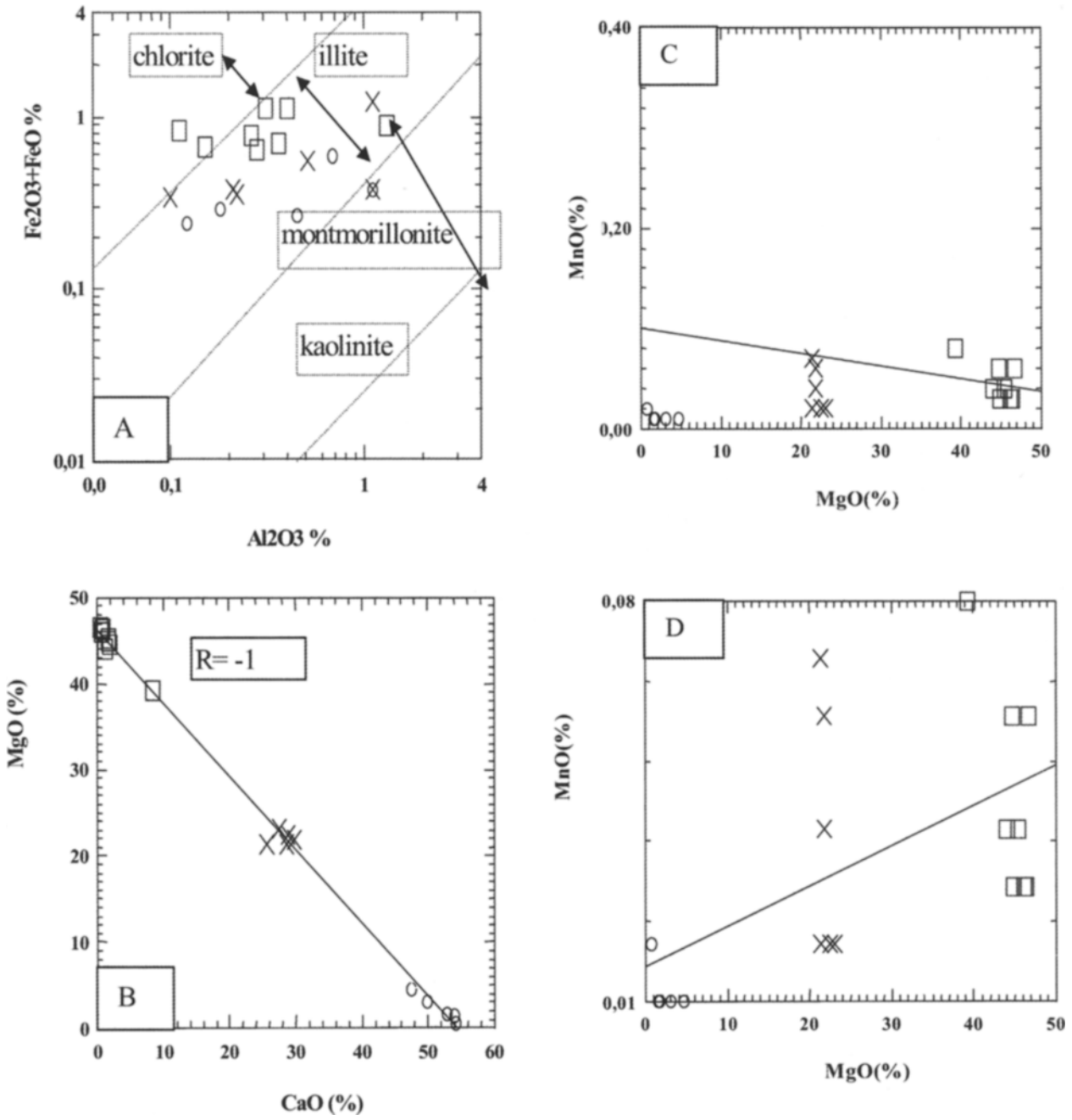

Figure 10. Scatter diagram for the studied carbonates. (A) Fe-Total vs. Al_2O_3 scatter diagram. The field for the clay minerals is from Deer et al. 1964 (in Veizer and Garret 1978). (B) MgO vs. CaO; (C) MnO vs. MgO; (D) MnO vs. MgO symbols as in Fig. 9.

process (e.g. Pohl and Siegl 1986), because Al and Si are tied to the clay fraction of the carbonate rocks while CaO gradually decreases from the calcitic to the magnesitic marbles.

Mn seems to decrease from the calcic marbles to magnesites (Fig. 10c). However, if we eliminate three samples corresponding to calcitic dolomitic marbles, a progressive Mn enrichment from the calcitic to the magnesitic marbles is observed (Fig 10d). According to Niedermayer et al. (1989), Fe and Mn contents are higher in continental or meteoric water than in seawater. Regarding that the dolomitic calcitic marbles represent brecciated material with calcitic cement, the abnormal concentrations in these rocks may be related to a secondary enrichment. On the other hand, in the normal sequence of the carbonate rocks, Fe^{3+} presents more irregularity and higher contents next to the magnesites. The enrichment of Fe_2O_3 and MnO next to the magnesitic marbles may be associated with the more soluble character of the Mn and Fe ions in an alkaline environment that makes them to precipitate together with Mg in more differentiated stages of the carbonate sequence.

Table 4. Correlation matrix for dolomitic marbles.

	CaO	MgO	Al_2O_3	Fe_2O_3	FeO	SiO_2	MnO	P_2O_5	TiO_2
TiO_2	-0.02	-0.09	0.78	0.71	0.56	0.26	0.22	0.97	
P_2O_5	0.07	-0.17	0.66	0.74	0.53	0.19	0.29		
MnO	0.93	-0.97	-0.12	0.40	0.44	-0.24			
SiO_2	-0.48	0.31	0.62	0.58	0.16				
FeO	0.16	-0.22	0.49	0.42					
Fe_2O_3	0.13	-0.29	0.67						
Al_2O_3	-0.39	0.26							
MgO	-0.98								

Table 5. Correlation matrix for calcitic marbles.

	CaO	MgO	Al_2O_3	Fe_2O_3	FeO	SiO_2	MnO	P_2O_5	TiO_2
TiO_2	-0.81	0.84	0.82	-0.19	0.61	0.44	-0.25	0.34	
P_2O_5	-0.25	0.28	0.40	-0.20	-0.04	-0.08	-0.39		
MnO	0.47	-0.59	-0.46	-0.49	0.61	-0.32			
SiO_2	-0.86	0.78	0.81	0.74	0.10				
FeO	-0.27	0.20	0.30	-0.56					
Fe_2O_3	-0.42	0.36	0.34						
Al_2O_3	-0.98	0.96							
MgO	-0.98								

It is also plausible to think that continental water may have carried these elements to the original depositional environment.

Mn varies, therefore, as a result of the evolution of Eh and pH. Under conditions of Eh and pH close to neutral, the Mn^{2+} ion remains in solution and is available to precipitate as a carbonate component. The MnO content of the limestones is lower than of the dolomites (Holland 1984). This suggests that Mn can be more soluble than Ca and as so should remain in solution and precipitate as MgO, independently from late mobilizations. Even so, Fe and Mn of carbonate rocks are succeptible to late mobilizations, either associated with diagenesis or with metamorphism. On the other hand, such rocks probably developed at the end of the Paleoproterozoic. In this era, the Fe and Mn behavior was different from today. In this regard, carbonates of the Paleoproterozoic (2.25 ± 0.25Ga) were far more Fe- and Mn-enriched than their phanerozoic analogues (e.g., Veizer et al. 1992).

The chemical variations and irregular dispersion of these elements within the carbonate rocks also suggest that the sedimentation ocurred under variable environmental conditions, at shallow depth. The presence of at least 4 thin layers of metapelites, intercalated with metadolomites in the Alencar region, described by Parente (1995), constitutes a further evidence.

With regard to the medium-grained magnesites, Parente (1995) observed that such rocks present a more irregular composition and the SiO_2, Al_2O_3, Fe_2O_3 and CaO contents are higher than in the sparry correspondents. According to Parente, SiO_2 ranges from 1.1 to 21.9 % (avg. 7.19%). Al_2O_3 oscillates from 0.1 to 4.5% (avg. 0.76%), Fe_2O_3 ranges from 1.5 to 4.5% (avg. 2.4%), CaO from 0.8 ato 10.1% (avg. 2.29%) and MgO varies from 75 to 95% (avg. 87.15%).

If the two magnesitic types of marbles are compared, it becomes evident that the sparry type is more Mg-enriched and less enriched in Si, Al_2 Fe^{3-} and Ca than the medium-grained type. In the medium-grained magnesites, these elements exhibit a more irregular distribution, while in the sparry magnesites their distribution is more regular. The dolomitic marbles are more Si^-, Al^-, Ca^- and Mn-enriched and less enriched in Mg, and in a less extent in Fe^{3+}, than the magnesitic marbles.

Rare-Earth Elements (REE)

The calcitic marbles display $\sum$REE from 6.4 to 23.47ppm, calcitic dolomitic marbles from 30.2 to 112.4ppm, dolomitic marbles from 11.3 to 20.6ppm and sparry magnesitic marbles, between 5.3 and 11.5ppm. The (La/Lu)N ratio decreases from the calcitic marbles (21.0-61.03) to magnesitic marbles (3.9-19.6), with the calcitic dolomitic marbles (4.6-28.6) and the dolomitic marbles (10.01 to 21.50) presenting intermediate values between these two lithological types, indicating a fractionation of light REE between these rocks.

Chondrite-normalized REE patterns (values from Evensen et al. 1978) display a more REE enrichment next to the brecciated calcitic dolomitic marbles and a progressive decrease of REE from the calcitic to the magnesitic marbles and a light heavy REE enrichment next to the sparry magnesitic marbles (Fig. 11). It is also observed a negative Eu anomaly (Eu/Eu* from 0.4 to 0.9 in the calcitic marbles; 0.6 to 0.7 in the calcitic dolomitic marbles; 0.5 to 0.9 in the dolomitic marbles and from 0.5 to 0.7 in the magnesitic ones) while Ce displays a slightly positive anomaly.

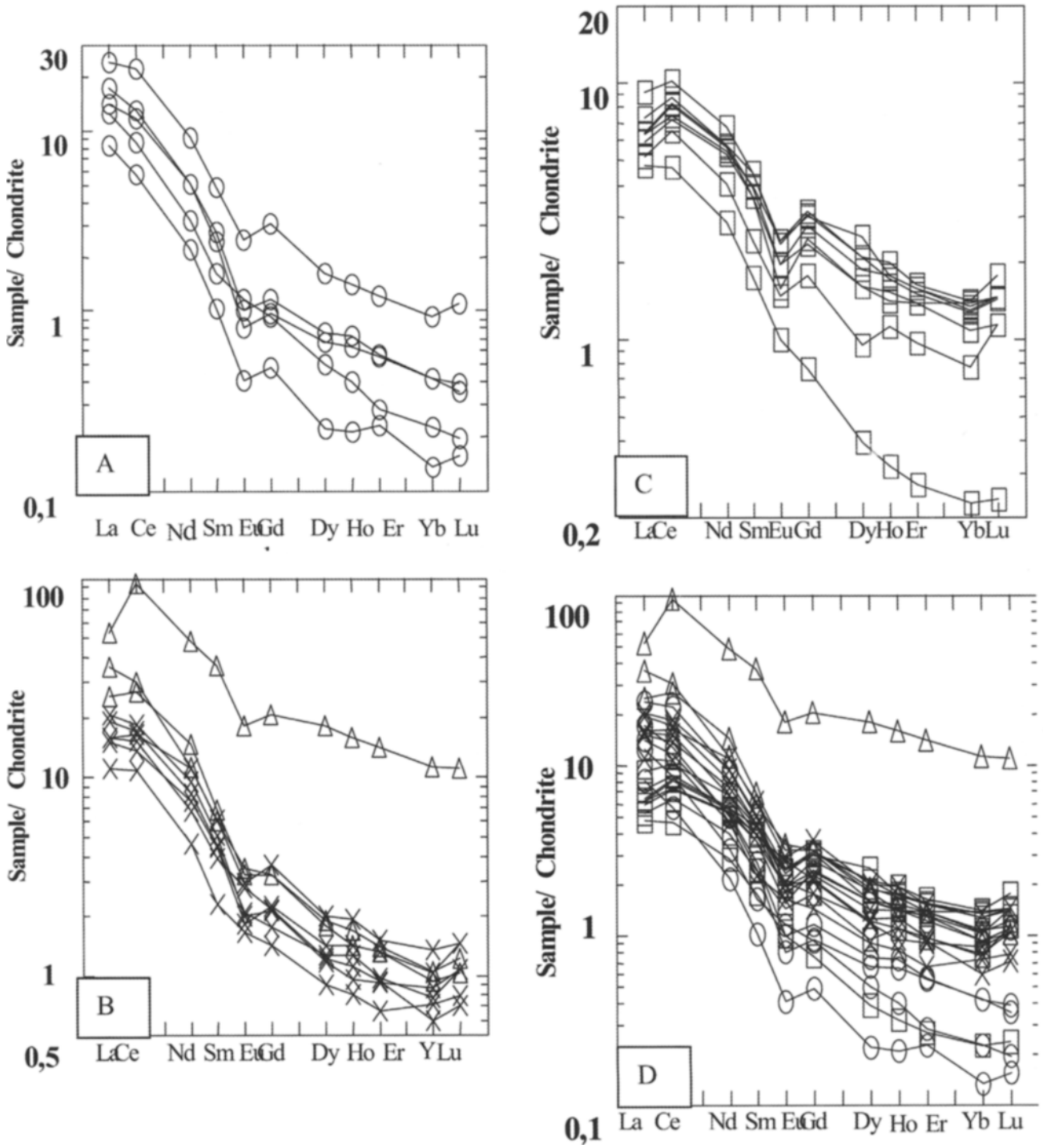

Figure 11. Chondrite-normalized rare-earth element patterns for marbles (normalizing factors are from Evensen et al. 1978). (A) Calcitic marbles; (B) Dolomitic marbles; (C) Sparry magnesitic marbles; (D) the studied metacarbonate rocks. Symbols as in Fig. 9.

Comparing these REE patterns to the pattern for the seawater, one observes that all the metacarbonate sequence presents a strong positive Ce anomaly and a weak positive Eu anomaly (Fig. 12).

In the calcitic marbles, REE display a significant negative correlation with CaO (r varies from -0.75 to -0.95) and a positive one in relation to MgO (r varies from 0.72 to 0.92) and with Al_2O_3 (r varies from 0.81 to 0.98). As Al_2O_3 varies sympathetically with SiO_2 and MgO and, to a lesser extent, with Fe_2O_3 indicating that the Al-silicate phase associated with the calcitic marbles is a magnesian chlorite with Fe, it is likely that REE can be associated with clay minerals rather than with the calcite of the calcitic marbles.

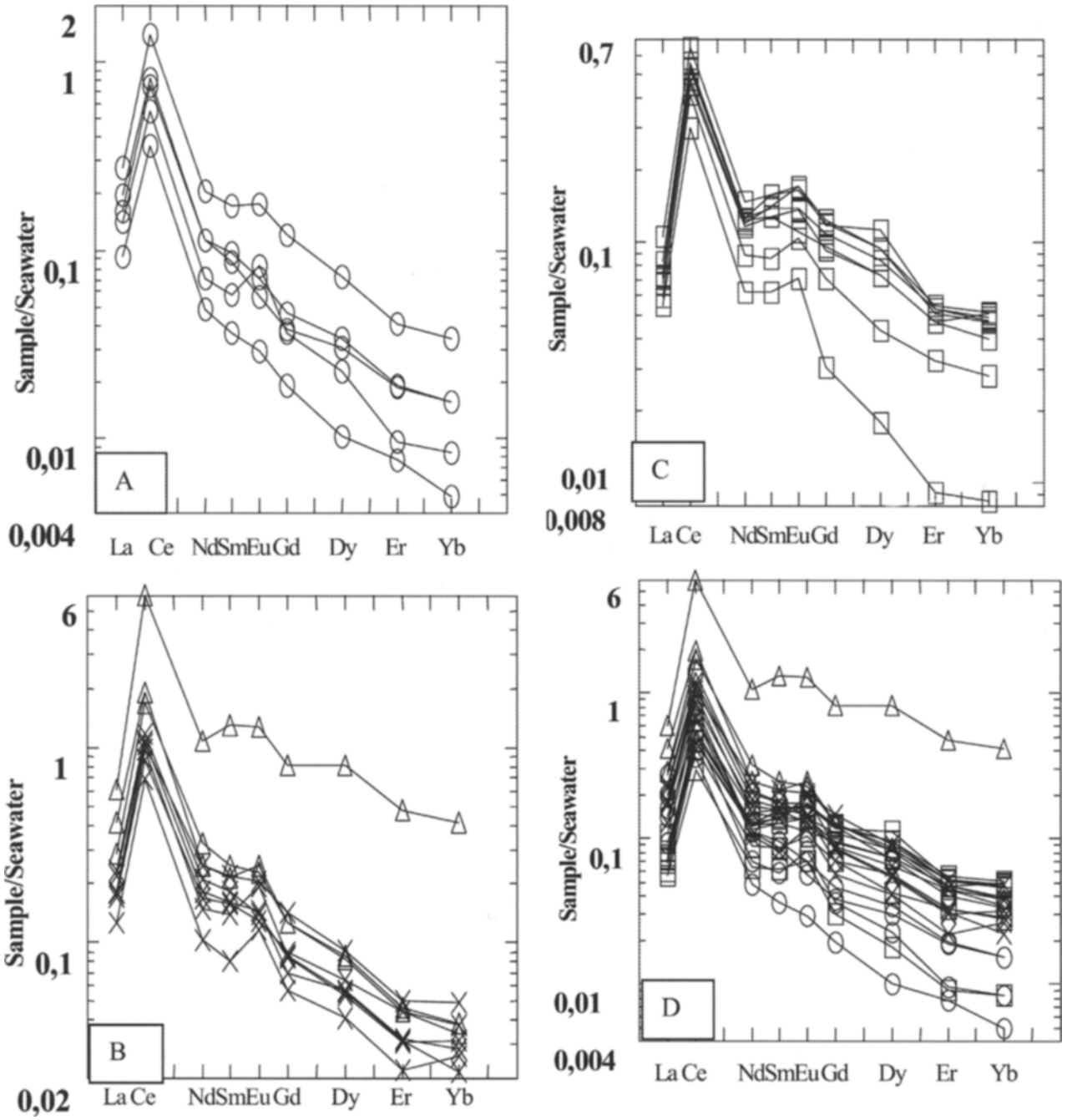

Figure 12. Seawater-normalized rare-earth element patterns for the studied marbles. (A) calcitic marbles; (b) dolomitic marbles; (c) magnesitic marbles; (d) the studied metacarbonate rocks. Symbols as in Fig. 9.

In the dolomitic marbles, there is no significant correlation between the REE and the major elements as for Mg and Ca (r é 0.6). However, the REE shows a weak positive correlation with Al_2O_3 and Fe_2O_3 (r varies, respectively, from 0.45 to 0.68 and from 0.72 to 0.78). La and Ce display a weak positive correlation with MnO (r =0.74 and 0.51 respectively) what suggests an affinity with Fe-Mn-oxide/hydroxide.

In the sparry magnesitic marbles, there is a weak negative correlation between REE and CaO (r = from -0.46 to –0.81) and MnO (r = -0.63 and –0.82), a positive one between REE and MgO (r = 0.5 to 0.75) and a poor correlation with Al_2O_3 (< 0.4) and with Fe_2O_3 (r = -0.16 and -0.42).

Regarding that REE concentrate particularly in the clay fraction of the carbonate rocks, it is likely that this difference in favor of the calcitic marbles can be tied to its less fractionated character than that of the dolomitic and magnesitic marbles. This would explain the observed differences in the behavior of the REE in the calcitic, dolomitic and magnestitic marbles.

Ce and Eu Anomalies

The knowledge of the behavior of these two elements is very useful in paleo-environmental reconstitution. The negative anomaly of Ce in sedimentary rocks, particularly in carbonate rocks, has been many times used to invoke a marine origin, due to its easier remotion in oxidation zone. In the oceans, Ce^{3+} is oxidized to Ce^{4+} that is soluble precipitating as CeO_2, resulting in a depletion of this element in the seawater in relation to the other REE (Elderfield and Graves 1982). As to the Ce positive anomaly, this could be related either to a reducing marine environment or to a shallow marine environment with influence of continental water (Tlig 1987). In the evaporitic lacustrine environment (Moller and Bau 1993), this anomaly is usually related to the negative Eu anomaly.

According to Fleet (1984) the lack of Ce depletion in marine sediments close to the coast (nearshore and coastal) could be associated with: (a) areas close to the continent, platformal regions, involving mixture between Ce-undepleted continental waters, that causes a more or less pronounced deficiency in Ce, influenced by formation of authigenic minerals near the coast; (b) areas of shallow seas, marginal basins to epicontinental, in which Ce is apparently in suspended solid particles with the remaining REE. In this case, even being tetravalent, Ce behaves just like the other REE.

In remote areas of the continents, this element is submitted to selective remotion within fine-grained solid particles (<0.1μm, Fe-Mn flakes). In consequence, Ce is separated from its neighbor elements (La and Nd) and a Ce anomaly may occur in the sediments.

This way, as pointed by Fleet (1984), it seems that seawater is not necessarily impoverished in Ce and that remotion of this element likely occurs in the open ocean rather than in platformal or estuarine waters. It should be also stressed that the absence of Ce anomaly in carbonate rocks is not due to diagenetic influence nor to dolomitization, but probably to formation of these rocks in environments with water not depleted in Ce.

Some authors admit, however, that marine sediments are depleted in Ce and consider that Ce depletion in modern oceanic waters is associated with the preferential incorporation of Ce^{4+} in authigenic minerals as Mn nodules and phosphorites (e.g. Piper 1974; McLennant et al. 1979).

Positive anomaly of Eu in the marine sediments or in seawater has been atributted to a hydrothermal inflow whose REE enrichment (e.g. Michard et al. 1983, Tlig 1987). This is typical of Archean sediments when primitive seas received a strong contribution of hydrothermal fluids. The negative anomaly of Eu is regarded as being characteristic of a reducing environment in which Eu^{3+} is reduced to Eu^{2+} although some authors have suggested that metamorphism or metasomatism could cause Eu reduction (e.g. Jarvis et al. 1975 in Fleet 1984).

Morteani et al. (1983), however, regard that the negative Eu anomaly is found in minerals formed from low-Eh solutions,while the positive Eu anomaly is ascribed to minerals formed in fluids with high oxygen fugacity, that interacted in the decomposition of feldspars. Möller (1989) considers that similar behavior of REE and the same types of negative anomalies of Ce and Eu between magnesites and dolomites is the product of magnesian metasomatism on dolomitic rocks. He also considers that the negative anomalies of Eu and Ce are associated, respectively, to a marine and to a reducing environment.

In the present case, a negative Eu anomaly and absence of a negative Ce anomaly may indicate that the studied magnesian carbonate sequence was developed in a paralic marine environment, platformal with euxinic influence. Metapelites intercalated in the dolomites of Alencar, dissolution breccias, mineral associations of evaporitic environment (Parente 1995; Parente et al. 1996) and hydrocarbon inclusions in magnesites, further support this contention. Perhaps REE were not in the seawater that equilibrated with Mn nodules, or there was no Mn nodule when the studied Mg carbonate sequence was deposited.

The REE patterns for the studied sparry magnesitic marbles keep some similarities to REE patterns obtained for petrographically equivalent Paleoproterozoic marbles of Liaodong,China (Fig. 13). However, some differences should be pointed out. The magnesian marbles of the Liadong province are more enriched in REE than those studied here and usually display Eu positive anomaly while those from Ceará, in Brazil, exhibit Eu negative anomaly. Magnesites of the Liadong province developed in the late Archean to early Paleoproterozoic (~2.5Ga), a time when there was more hydrothermal fluid inflow in the primitive ocean water, implying in a REE enrichment and in a Eu positive anomaly. Although there are some divergences, the available data altogether suggest that these two associations were developed in similar platformal environments and that the magnesitic rocks, mainly the sparry ones, are chiefly of sedimentary origin.

FLUID INCLUSIONS

Twenty two polished sections of dolomitic, sparry magnesitic and medium-grained marbles were examined for fluid inclusion studies. However, only in magnesite from the Riacho Fundo and Cabeça de Negro deposits, fluid inclusions with size, transparency and in adequate amount for a detailed study, were found. From the petrographic study, fluid inclusions have been classified and a detailed study of microthermometry and Raman microspectrometry was carried out. A Dilor multichannel Raman spectrometer

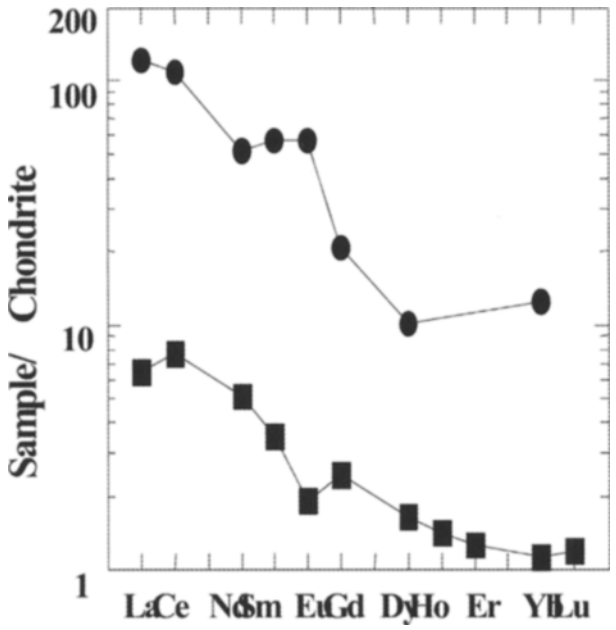

Figure 13. Rare earth-element distribution showing the average for the magnesitic marbles of the Liadong province (circles, average of 11 samples) and for the chondrite-normalized Cabeça de Negro deposit (squares; average of 8 samples). Normalizing factors are from Evensen et al. (1978). Data from Quisheng (1988).

from the Physics Institute of the Federal University of Minas Gerais was used. A Chaix Meca stage of the fluid inclusions laboratory of the Vale do Rio dos Sinos University (Poty et al. 1976) that allows temperature measurements between –180°C and +600°C with reproducibility of +0.2°C was used. The calibration curve was prepared with pure H_2O-CO_2 fluid inclusions, deionized water and Merck solid products of known melting point.

Medium-Grained Magnesite from Riacho Fundo

There are several types of fluid and solid inclusions in the medium-grained magnesite of the Riacho Fundo deposit, some of which display a regular distribution as shown in Fig. 14. In the first place, we see a light zone without fluid or solid inclusions (number 1 in Fig. 14). Next, we have a narrow zone with biphasic aqueous (aqueous LC, 2 in Fig. 14) with polygonal shapes, walls parallel to the growth walls and size that can reach 30 μm. Eventually, one can see monophasic aqueous inclusions associated with the biphasic group, probably a metastable process. There is a third central zone (AC type, 3 in Fig. 14) much wider that displays solid inclusions, normally rounded to oval, of dolomites (determined by Raman spectrometry), aquo-carbonic inclusions with or without associated dolomite. The size and shape of these inclusions are variable and could reach up to 30 μm. Their distribution is aleatory, being roughly parallel to the growth lines of magnesite. Finally, one repeats the narrow zone 2 with aqueous biphasic inclusions and the first zone without solid or fluid inclusion. This distribution of the inclusions probably reflects the process of growth of the magnesite crystal during a metamorphic recrystallization, implying in that these fluid inclusions are primary in relation to the metamorphic process.

One fluid inclusion of the LC type (liquid aqueous) revealed traces of CO_2 and N_2 in the Raman spectrometry, while in the aquo-carbonic inclusions, only CO_2 was detected, although CH_4 and N_2 were also investigated. A third type of inclusion, partially or totally filled by an opaque, black material that may form rounded inclusions with small light aqueous appendices, that is usually associated with rounded solid inclusions of dolomites (Fig. 15). The size of the black phase is less than 5 μm and its composition could not be determined by Raman spectrometry due to a high fluorescence generated during the analysis that maskes completely the Raman signal (Pironon et al. 1991). This behavior is characteristic of inclusions with hydrocarbon. The carbon peaks are of 1300 and 1580 cm^{-1} and according to McMillan (1989) graphite has two sharp peaks (1582 and 140cm^{-1}) well marked in Raman spectrometry without

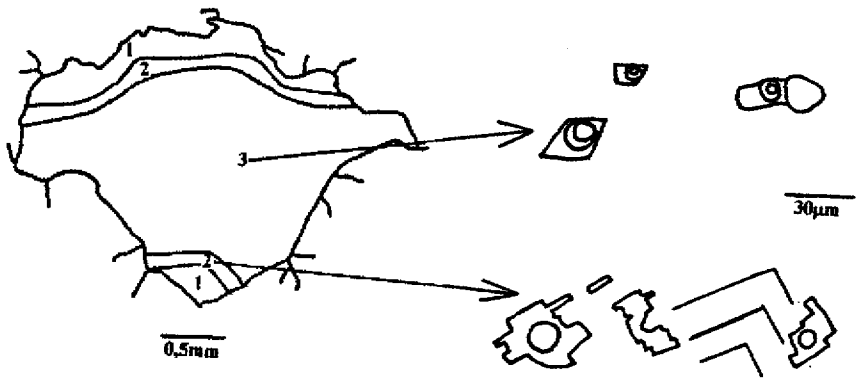

Figure 14. Magnesite crystal (left) with growth lines and three bands without and with different types of fluid inclusions that, by their turn, are schematically shown to the left: 1. Clean band without inclusions; 2. Biphasic fluid inclusions and aqueous monophasic, the straight lines at an angle representing growth lines; 3. Aquo-carbonic inclusions with and without dolomite as accidental solid.

Figure 15. (A) Rounded solid of dolomite with a black portion of probably hydrocarbon and associated aqueous portion. (B) Inclusions with hydrocarbon and aqueous appendices. A little trail of aqueous inclusions and the occurrence of monophasic and biphasic inclusions apparently associated with inclusions with hydrocarbon.

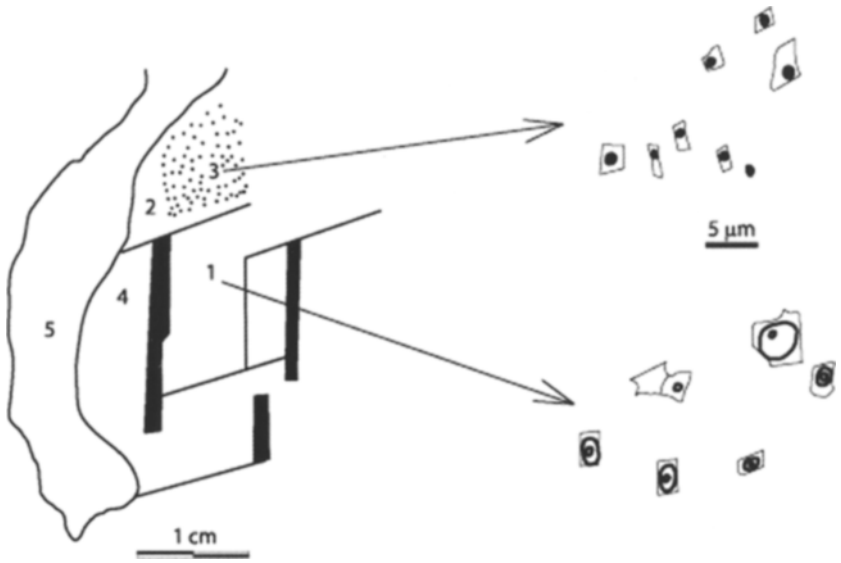

Figure 16. Main kinds of fluid inclusions found in sparry magnesite from the Cabeça de Negro Deposit: 1. aqueous-carbonic inclusions, probably secondary; 2. Fluid-inclusion-free magnesite zone; 3. Biphasic aqueous fluid-inclusion-zone, probably primary; 4. Secondary monophasic and biphasic fluid inclusions; 5. Fine-grained white inclusion-free magnesite.

fluorescence. Its composition could only be determined with infrared microspectrometry, if its size were larger than 15 μm which is not the case (Pironon et al. 1991). The pasty nature was evidenced during the exposure to the laser beam, when a small hole was formed and that expontaneously closed again after some weeks.

Besides these inclusions, probably primary in relation to the metamorphism, one has another very small aqueous, monophasic and biphasic, inclusions (< 5 micrometers) in secondary trails.

Sparry Magnesite from Cabeça de Negro Deposit

In this type of sparry magnesite, one found fluid inclusions similar to those described in the Riacho Fundo deposit, at different proportions. Whereas in the Riacho Fundo deposit aqueous inclusions predominate, in the Cabeça de Negro deposit aquo-carbonic inclusions predominate. Even so, it is evident that the occurrence of these two types of fluid inclusions are in neighbor crystals. The Fig. 16 is a typical example of what happens in this sample where we have a longitudinal trail with aquo-carbonic inclusions (AC type, 1 in Fig. 16) restrict to a single crystal and probably pseudo-secondary. In the neighbor crystal, two well limited zones, one clean without any type of inclusion (2 in Fig. 16) and another with aqueous inclusions (type LC) in the form of negative crystals with aleatory distribution and possibly primary, are observed. The trail marked as 4 in the same Fig.16, transversal to a tabular crystal of magnesite is composed by tiny (<2 μm) inclusions apparently aqueous monophasic, biphasic and secondary, once the trail cuts

more than one crystal. In five of them, one has a fine, white, translucid magnesite mass, without fluid inclusions. In general, there is very little solid inclusions of dolomite or with hydrocarbons.

ISOTOPIC GEOCHEMISTRY

Carbon and oxygen isotopes were analyzed in sixteen samples of calcitic and dolomitic marbles at the stable isotope laboratory (LABISE) of the Federal University of Pernambuco. About 10 to 20 mg of powdered sample have been put to react with 100% orthophosphoric acid at 25°C. CO_2 released from this reaction was cryogenically purified to remove water, that results from the reaction of the carbonate with the orthophosphoric acid, and analyzed for C and O isotopes in a VG ISOTECH SIRA II dual inlet, triple collector mass spectrometer, using the BSC (Borborema skarn calcite) as the reference gas that was calibrated against international standards (NBS-18, NBS-19, NBS-20). Results are expressed in notation (Table 6).

These metacarbonates exhibit $^{13}C_{PDB}$ values from -3.2 to +2.1‰. Such a variation may reflect modification occurred during metamorphism or the original isotope values acquired during the sedimentation of these carbonates. As these rocks underwent metamorphism in the greenschist to low amphibolite facies, probably did not go through decarbonation reactions that would have caused isotopic changes (Hoefs 1997). Therefore, the carbon-isotope values can be used to estimate environmental conditions during deposition of the carbonates. In this case, calcitic marbles display $^{13}C_{PDB}$ from +0.5 to +2.1‰ a range typical for open sea environment while calcitic dolomitic marbles, with values between –0.51 and - 3.14‰, could have been deposited in brackish or confined marine environmemnt with strong continental influence. This data set is also in agreement with ^{13}C fluctuations observed in late Paleoproterozoic carbonates (~1.8Ga; e.g. Veizer et al. 1992; Sial et al. 2000).

The $^{18}O_{PDB}$ values for the calcitic marbles vary from -6.6 to -10.3‰$_{PDB}$ while for the dolomitic marbles vary from -9.4 to -14.8‰ $_{PDB}$. The oxygen isotope ratios are more susceptible to modifications during metamorphism, even at a low degree, in a way they are of little use to trace the thermal history of deposition of the carbonates. However, the highest values, which are associated with the salmon red dolomitic marbles (CMMD-6G) and pink dolomitic marbles (CMMD-6H), could represent the least altered dolomitic rocks or formed in shallower marine water, while those of lower oxygen isotope values may indicate oxygen mobility during metamorphism or a deeper marine environment.

GENETIC MODEL

A difficult problem in the study of magnesite deposits associated with metasedimentary rocks is to determine whether these deposits are metasedimentary or metasomatic rocks.

In this study, the presence of two types of magnesite of different grain size poses an interesting problem. It is known that, in general, grain size of the carbonates is linked to the concentration of ions and to the salinity of the environment (Folk and Land 1975; Guillou 1980). Two processes are common: co-precipitation and maturation of the precipitate.

Co-precipitation is a chemical precipitation related to

Table 6. C and O isotope analyses (‰) for calcitic and dolomitic marbles.

Samples	$\delta^{18}O_{SMOW}$	$\delta^{18}O_{PDB}$	$\delta^{13}C_{PDB}$
CMMD-1M – white calcitic marble	+21.5	-9.0	+0.5
CMMD-1N – light gray calcitic marble	+23.9	-6.6	+2.0
CMMD-1P - white calcitic marble	+20.2	-10.3	+1.9
CMMD-5A – light gray calcitic marble	+21.7	-8.8	+1.0
CMMD-5B – light gray calcitic marble	+21.1	-9.3	-0.5
CMMD-6C – buff dolomitic marble	+21.1	-9.4	-2.3
CMMD-6D – pink dolomitic marble	+16.7	-13.6	-0.9
CMMD-7F – buff dolomitic marble	+15.5	-14.8	-0.7
CMMD-8I – gray dolomitic marble	+16.0	-14.4	-1.1
CMMD-8J – gray dolomitic marble	+16.3	-14.1	-1.1
CMMD-8L – gray dolomitic marble	+17.6	-12.8	-1.2
CMMD-6B – pink dolomitic calcitic marble	+18.5	-11.9	-1.5
CMMD-6E – buff dolomitic marble	+16.3	-14.0	-1.0
CMMD-6F - pink dolomitic calcitic marble	+16.2	-14.1	-3.1
CMMD-6G – salmon red dolomitic marble	+28.8	-1.9	-1.1
CMMD-6H – pink dolomitic marble	+25.1	-5.5	-0.8

the presence of impurities. These impuritise can be adsorbed or hidden in the structure of the host mineral during the crystallization stage. This process happens in supersaturated environment rich in impurities where crystallization is rapid (Catani et al. 1970 in Almeida 1989). This way, in a strongly saturated evaporitic environment, germs are numerous, crystallization is fast and sediments will evolve little, preserving fine-grain size. Folk and Land (1975) showed that the formation of ordered dolomite is inhibited, at the same time, by the rapidity of the crystallization process in an oversaturated medium and by the concentration of strange ions in this process.

Maturation of the precipitate, by its turn, is related to the more diluted solution, weakly oversaturated where germs are more rare. The strange ions, due to their longer time in solution are eliminated, leaving only two dominant ions (Catani et al. 1970 in Almeida 1989). The crystallization is slow and the sedimentary evolution is faster and this allows for larger, well-defined crystals (Guillou 1980). Folk and Land (1975) pointed out that in the mixing zone of marine and freshwater (schizohaline zone) or of reduced salinity, dolomite crystals are larger and cleaner than those ones formed in an oversaturated environment.

Therefore, it is plausible to assume that the two types of magnesite studied developed in environment with different confining or salinity index: medium-grained magnesitic marbles would have been formed in a more confined or saturated environment than the sparry magnesitic marbles, where the influence of freshwater able to modify the salinity of the original environment was negligible. Abundant pyrite inclusions in subrounded magnesite, a result from bacterial activity in a saline or hypersaline environment, is a further support to this idea. Sparry magnesitic marbles were developed in a paralic, lagunar environment, less saturated than the former and wherein ion concentration was similar to that of seawater, taking into account the balance between evaporation and influence of freshwater inflows. This allowed a slower carbonate crystallization accompanied by important diagenetic processes, responsible for the crystallographic evolution. The common association between red, ferruginous, sparry magnesites and Fe-enriched metadolomites, Al-silicates and detrital zircons are an indication of a strong contribution of freshwater to these deposits.

Most investigations on the formation of magnesite in recent sedimentary environment have shown that the $Ca^{2+}/(Ca^{2+}+ Mg^{2+})$ decrease in the carbonate rocks in the paralic systems from open sea to landwards, that is, one goes from more calcic in open sea to more magnesian in confined environment. The Ca^{2+} decrease could be related to initial crystallization of calcic carbonates or gypsum or both (Müller et al. 1972; Von der Borg 1965, 1976).

In ancient environments, this differentiation was already demonstrated by Guillou (1980) in Cambrian rocks in Spain (Pacios and Mallecina) whose sequence dominated by dolomitic and magnesitic carbonates developed progressively from open sea to lagunar environment. In this study, we found one of the alternatives proposed by Guillou (1980), that is, magnesites are found in the central part in a paleo-lagoon and not in marginal positions as in the Spanish Cambrian. Guillou (1980) also associated the decrease and disappearance of sparry magnesite, to the atmospheric fCO_2 decrease by the action of carbon-intaker organisms. The CO_2 decrease is today accepted by unanimity. One can also think on Ca solubility that, compared to that for Mg, increases with the elevation of pCO_2.

Another worth-mentioning point is that the hypermagnesian carbonates are more resistant to tectonic deformation and pressure solution than their calcic analogues. Once submitted to deformation and metamorphism, magnesian carbonates resist more to ion exchange than the calcic carbonates. In a metasomatic hypothesis, where it is assumed that the introduction of Mg^{2+} was during metamorphism limestones or dolomites, the magnesite and its precursor dolomite would have a similar signature of trace elements of little mobility like Al. The sparry magnesitic marbles and host metadolomites exibit important differences in Al_2O_3, Fe_2O_3 and MnO and, therefore, a large-scale metasomatism cannot explain these differences that are probably related to simple sedimentary phenomena, such as progressive depuration of lagunar water from clays (Al_2O_3 and SiO_2) and, on the contrary, its Fe^{2+} enrichment, very stable at the time of formation of these rocks. Besides, three other facts are in support of a sedimentary origin: (a) abundant dolomitic and ferriferous magnesitic marbles as well as detrital zircon in the host metadolomites; (b) red dissolution breccias (evaporite dissolution) with lutecite, sulphate nodules pseudomorphosed by fiber-radiated quartz in the contact between metadolomites and magnesites, and also presence of scapolite that indicates evaporitic conditions. In this case, the early saline fraction would have been partially dissolved during the emersion stage in oxidizing conditions since pseudomorphosed sulphate nodules are still observed; (c) dissolution breccias and thin films of metapelite, within the metadolomites, suggest a hiatus in the carbonate sedimentation.

The studied magnesites are in a border of an emerging zone, submitted to a pronounced alteration, but subjected to a reduced erosion under climatic conditions that vary from humid to arid. It is well known that under arid climate, evolved aluminous and detrital inflows characterize the sedimentary context. Therefore, it is possible to assume that periodical inflows of continental freshwater brought Fe and heavy minerals during the formation of magnesite. Dolomites are situated in large intra-deltaic paralic depressions (lagoons). Limestones are more distal and correspond to more open marine environments. Altogether, these carbonates appear during periods of weak erosion,

under arid climate and evaporites fit well in this context. Besides, occurrence of organic matter (oil in particular) suggests a biological activity in a confined medium.

As a whole, the present data seem more consistent with a sedimentary hypothesis than to metasomatism. The latter does not explain the granulometric variations observed in the studied magnesites, developed in environments relative close to each other.

Finally, regarding that the set of magnesite occurrences passes, westward, through metadolomites into almost pure calcitic marbles, the chemical differentiation model proposed by Guillou (1971, 1980) and Chayé d'Albissin and Guillou (1986, 1988) in which the sparry magnesite appears towards the end of the carbonated chain, can be invoked to explain it. In the present case, this model envolves an epicontinental marine gulf paleogeography, where the lagunar water loses Ca, from west to east, by preferential precipitation of calcic carbonates and further, in a more arid climate, gypsum was precipitated, raising its Mg/Ca ratio, driving the carbonate evolution toward the magnesian pole. The Figure 1 presents a scheme of the paleogeography and Figure 17 synthetizes the studied magnesian carbonate sequence evolution.

CONCLUSIONS

The geological, geochemical and fluid inclusion study of this magnesian carbonate sequence of the Orós foldbelt show two types of magnesite (sparry and of medium-grain size) of dominantly sedimentary origin.

The textural and compositional variations in the magnesite domain indicate that such rocks developed in different environments. The sparry magnesite formed in a paralic environment, weakly saturated wherein the germs were rare, slow crystallization and important diagenetic

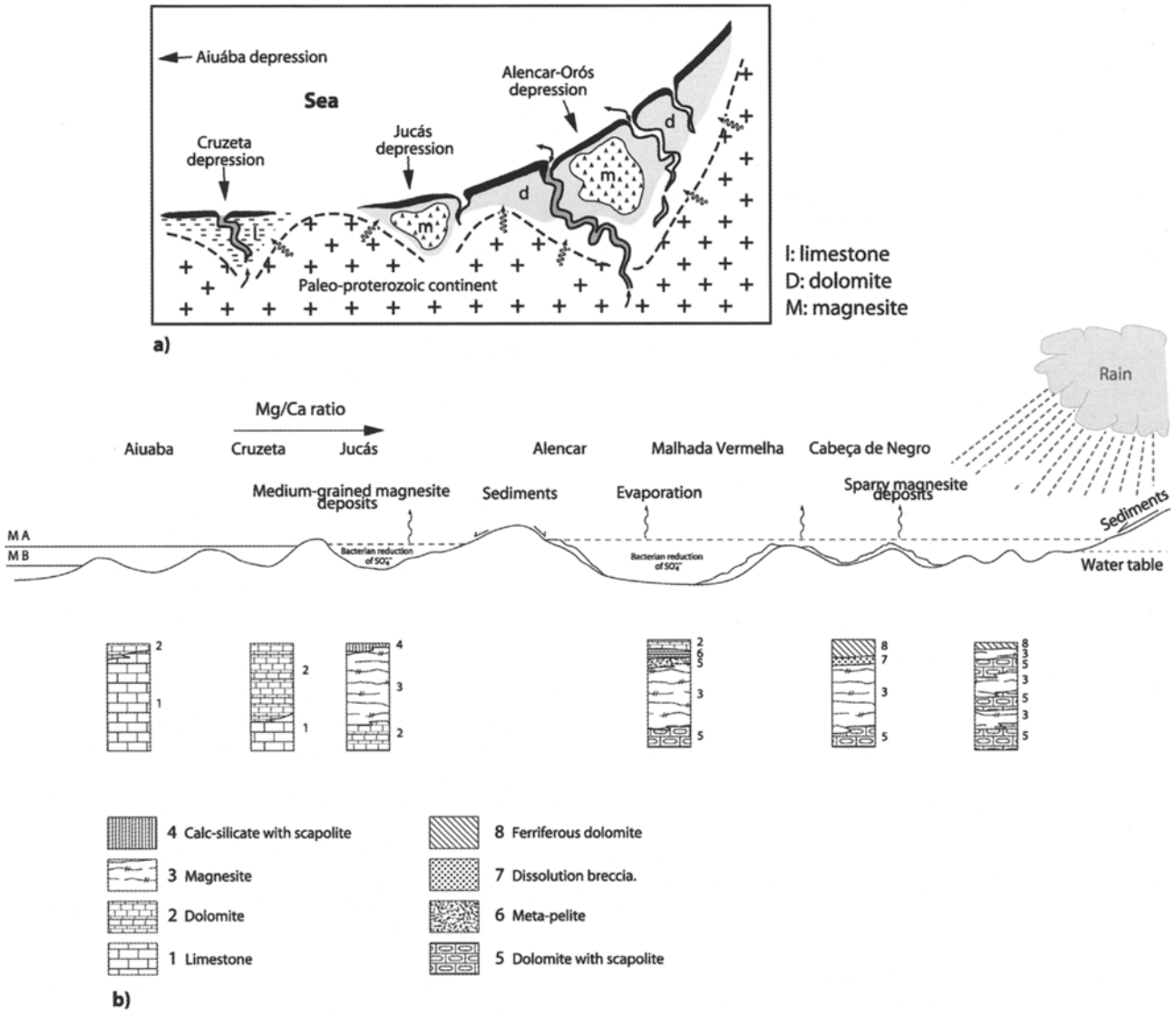

Figure 17. Paleogeographic (a) and interpretative (b) scheme for the magnesian carbonate sequence of Ceará, NW Brazil.

evolution. Magnesites of medium-grain size developed in the same paralic environment, but more confined and/or saturated than that of the sparry magnesite. The greater concentration of ions of different composition associated with the magnesian ions favor a rapid crystallization and a lesser diagenetic evolution.

The distribution of the aqueous and aquo-carbonic fluid inclusions in both magnesite deposits indicate that these fluid inclusions are primary in relation to the tectono-metamorphic event, reflecting magnesite crystal growth during the metamorphism.

We can reconstitute the paleogeography, probably diachronic, configuring a series of paralic gulfs where evaporitic associations mix with continental influences. In this model, the magnesite deposits seem to be situated in the middle of two main paralic gulfs, both in distal position in relation to the sea. The sparry magesite deposit was formed in the largest and more distal one in a more stable environment than that for the medium-grained magnesites.

This model confirms the major lines of previously analyzed cases, especially regarding Ca and Mg segregations in a sea-continent gradient; ratifies the existing data about the formation of other magnesite deposits and underlines the originality of the supergenic domain in the formation of evaporitic and carbonatic deposits, in the Proterozoic, marked by a strong pCO_2.

ACKNOWLEDGEMENTS

CVP wishes to thank the IBAR Mining and FUNCAP (proc. 110/95) for financial support, field work and laboratory analyses. We want to express our gratitude to Donald Clark and German Müller whose critical review greately improved the original manuscript.

REFERENCES

AHARON, P., 1988, A stable-isotope study of magnesites from the Rum Jungle Uranium Field. Australia: implications for the origin of strata-bound massive magnesites: *Chemical Geology*, v. 69, p. 127-145.

ALMEIDA, T.I.R.,1989, Magnesita do depósito de Campo de Dentro. Serra das Éguas. Bahia: Geoquímica e gênese. Tese de doutoramento da Universidade de São Paulo. Instituto de Geociências (unpublished), 173 p.

ARBEY, F., 1980, Les formes de la silice et l'identification des évaporites dans les formations silicifiées: *Bull. des Centres de Rech. Expl.-Prod. Elf-Aquitaine*, v. 4, p. 309-365.

BADHAM, J.P.N. and STANWORTH, C.W., 1977, Evaporites from the lower Proterozoic of the East Arm. Great Slave Lake: *Nature*, v. 268, p. 516-518.

BODENLOS, A.J., 1948, Magnesite deposits of Ceara Brazil: *U.S.Geological Survey Bulletin*, no. 062-C, p. 121-151.

BODENLOS, A.J., 1954, Magnesite deposits in the Serra das Eguas. Brumado. Bahia. Brazil: *U.S.Geological Survey Bulletin*, no. 975L, p. 87-170.

BONE, Y., 1983, Interpretation of magnesites at Rum Jungle. N.T.. using fluid inclusions: *Journal of the Geological Soc. Australia*, v. 30, p. 375-381.

BUSSON, G. and PERTHUISOT, J.P., 1977, Intérêt de la Sebkha El Melah (sud-Tunisien) pour l'interprétation des séries évaporitiques anciennes: *Sedimentary Geology*, v. 19, p. 139-164.

CHAYE D'ALBISSIN, M. and GUILLOU, J.J., 1986, Evolution cristallogénétique de magnésites spathiques antéjurassiques. du stade sédimentaire à la mésozone. Exemples comparés de Gumpa-de-Bigu (Népal) et de Pacios (Espagne): *Revue de Géologie Dynamique et de Géographie Physique*, v. 27, p. 339-349.

CHAYE D'ALBISSIN, M. and GUILLOU, J.J., 1988, Conditions de genèse et comportement mécanique des magnésites spathiques antéjurassiques au cours de leur histoire géologique: *Bull. Soc. Géol. France*, v. t.IV, p. 871-877.

ELDERFIELD, H. and GRAVES, M., 1982, The rare earth elements in seawater: *Nature*, v. 296, p. 214-219.

EVENSEN, N.M., HAMILTON, P.J., and ONIONS, R.K., 1978, Rare-earth abundance in chondritic meteorites: *Geochim. Cosmochim. Acta*, v. 31, p. 1637-1665

FLEET, A.J., 1984, Aqueous and sedimentary geochemistry of the rare earth elements. *In* P. Henderson and W.S. Fyfe, eds., Rare Earth Geochemistry. Elsevier, Amsterdam, p. 343-373.

FOLK, R.L. and LAND, L.S., 1975, Mg/Ca Ratio and Salinity: two controls over crystallization of dolomite: *AAPG Bulletin*, v. 59, p. 60-68.

FRIEDMAN, G.M., 1980, Dolomite is an evaporite mineral: Evidence from the rock record and from sea-marginal ponds of Red Sea. *In* D.H. Zenger, J.B. Dunham, and R.L. Ethington, eds., Concepts and Models of Dolomitization: SEPM Special Publication no. 28.

FRIEDMAN, G.M. and SHUKLA, V., 1980, Significance of authigenic quartz euhedra after sulfates: example from the Lockport Formation (Middle Silurian) of New York: *Journal of Sedimentary Petrology*, v. 50, p. 1299-1304.

GOMEZ DE LLARENA, J.G., 1968, La diagénesis en la dolomita y magnesita de Asturreta (Eugui. Navarra): un problema por estudiar: *Bol. R. Soc. Española Hist. Nat. (Geol.)*, v. 66, p. 41-48.

GUILLOU, J.J., 1972, La série carbonatée magnésienne et l'évolution de la composition de l'hydrosphère: *C. R. Ac. Sc. Paris*, v. 274, p. 2952-2955.

GUILLOU, J.J., 1973, Les concentrations magnésiennes silicatées en contexte métamorphique: apport métasomatique ou préexistence ?: *C. R. Ac. Sc. Paris*, v. 276, p. 149-151.

GUILLOU, J.J., 1980, Contribution à la métallogénie des magnésitites. exemple du Cambrien Espagnol. Thèse de Doctorat d'Etat de l'Université Pierre et Marie Curie (Paris 6), 155 p.

GUILLOU, J.J. and LETOLLE, R., 1988, Origine mixte chimique et biochimique des dépôts de magnésite antérieurs au Jurassique en milieu marin confiné. marginal-littoral: *C.R. Acad. Sc. Paris*, v. 303, Série II, p. 207-212.

HIETANEN, A., 1967, Scapolite in the Belt Series in the St. Joe-Clearwater Region. Idaho: GSA Special Paper, v. 86, p. 1-56.

HOEFS, J., 1997, Stable Isotope Geochemistry. Ed. Springer-Verlag, 201 p.

HOGARTH, D.D. and GRIFFIN, W.L., 1978, Lapis lazuli from Baffin Island - a Precambrian meta-evaporite: *Lithos*, v. 11,

p. 37-60.

HOLLAND, H.D., 1984, The chemical evolution of the atmosphere and oceans. Ed. Princeton University Press, Princeton, N.J., 582 p.

JOSHI, M.N., BHATTACHARYA, A.K., and ANATHARAMAN, M.S., 1993, Origin of the sparry magnesite deposits around Bauri. Almora district. Uttar Pradesh. India: *Mineral Deposita*, v. 28, p. 146-152.

KRALIK, M., AHARON, P., SCHROLL, E., and ZACHMANN, D., 1989, Carbon and oxygen isotope systematics of magnesites: a review: *Monograph Series Mineral Deposits*, v. 28, p. 197-223.

LEAKE, B.E. and FARROW, C.M., 1979, A pre-2000 Myr old granulite facies metamorphosed evaporite from Caraiba. Brazil: *Nature*, v. 277, p. 49-50.

LUGLI, S., TORRES-RUIZ, J., GARUTI, G., and OLMEDO, F., 2000, Petrography and Geochemistry of the Eugui Magnesite Deposit (Western Pyrenees. Spain): Evidence for the development of a peculiar zebra banding by dolomite replacement: *Economic Geology*, v. 95, p. 1775-1791.

MCLENNANT, S.M., FREYER, B.J., and YOUNG, G.M., 1979, The geochemistry of the carbonate rich Espanhola Formation (huronian) with emphasis on the rare earth elements: *Can. J. Earth Sci.*, v. 16, p. 230-239.

MCMILLAN, P.F., 1989, Raman spectroscopy in mineralogy and geochemistry. Ann. Ver.: *Earth Planet. Sci.*, v. 17, p. 255-283.

MELEZHIK, V.A., FALLICK, A.E., MAKARIKHIN,V.V., and IYUBTOV,V.V., 1997, Links between Paleoproterozoic paleogeography and rise and decline of stromatolites: Fennoscandian Shield: *Precambrian Research*, v. 82, p. 311-348.

MELEZHIK, V.A., FALLICK, A., MEDVEDEY, P.V., and MAKARIKHIN, V.V., 2001, Paleoproterozoic magnesite: lithological and isotopic evidence for playa/sabkha environments: *Sedimentology*, v. 48, p. 379-397.

MENDONÇA, J.C.G.S. and BRAGA, A.P.G., 1987, As faixas vulcano-sedimentares de Orós-Jaguaribe: um greenstone belt?: *Revista Brasileira de Geociências*, v. 17, p. 225-241.

MICHARD, A., ALBAREDE, F., MICHARD, G., MONSTER, J.F., and CHARLOUS, J.L., 1983, Rare-earth elements and uranium in high-temperature solutions from East Pacific Rise hydrothermal vent field (13°N): *Nature*, v. 303, p. 795-797.

MÖLLER, P., 1989, Minor and trace elements in magnesite: *Monograph Series Mineral Deposits*, v. 28, p. 173-195.

MORTEANI, G., 1989, Mg-metasomatic type sparry magnesites of Entachen Alm, Hochfilzen/Bürglkopf and Spiessnägel (Austria): *Monograph Series, Mineral Deposits*, v. 28, p. 105-113.

MORTEANI, G., MÖLLER, P., and SCHLEY, F., 1982, The Rare Earth Element contents and the origin of the sparry magnesite mineralizations of Tux-Lanersbach. Entachen Alm, Spiessnagel, and Hochfilzen. Austria. and the lacustrine magnesite deposits of Aiani-Kozani. Greece. and Bela Stena. Yugoslavia: *Economic Geology*, v. 77, p. 617-631.

MORTEANI, G., SCHLEY, F., and MÖLLE, P., 1983, On the formation of magnesite. *In* H.J. Schneider, ed., Mineral Deposits of the Alps and of the Alpine Epoch in Europe. Springer-Verlag, Berlin Heidelberg, p. 105-116.

MULLER, G., IRION, G., and FORSTNER, U., 1972, Formation and diagenesis of inorganic Ca-Mg Carbonates in the Lacustrine Environment: *Naturwissenchaften*, v. 59, p. 158-164.

NIEDERMAYR, G., BERAN, A., and BRANDSTATTER, F., 1989, Diagenetic type magnesites in the Permo-Scythian rocks of the Eastern Alps. Austria: *Monograph Series Mineral Deposits*, v. 28, p. 35-59.

NISHIHARA, H., 1956, Origin of the bedded magnesite deposits of Manchuria: *Economic Geology*, v. 4, p. 698-711.

PAPAIOANOU, F.P. and CAROTSIERIS, Z., 1993, Dolomitization patterns in Jurassic-Cretaceous dissolution - collapse breccias of Mainalon Montain (Tripolis Unit. Central Peloponnesus - Greece): *Carbonates and Evaporites*, v. 8, p. 9-22.

PARENTE, C.V., 1995, Géologie et paléogégraphie d'une plate-forme à évaporites et magnésite d'âge protérozoique (2 Ga): le cadre géotectonique initial de la ceinture mobile Orós dans la région d'Alencar (Ceará-Brésil). Thèse de Doctorat de l'Université de Nantes, 306 p. (unpublished).

PARENTE, C.V. and ARTHAUD, M.H., 1995, O Sistema Orós-Jaguaribe no Ceará-NE do Brasil: *Revista Brasileira de Geociências*, v. 25, p. 297-305.

PARENTE, C.V., GUILLOU, J.J., and BARBOSA, H.S., 1996, Evaporitos pré-cambrianos (~1.8Ga) da Faixa Orós. Ceará (Brasil): *Revista de Geologia*, v. 9, p. 5-16.

PIPER, D.Z., 1974, Rare earth elements in ferromanganese nodules and other marine phases: *Geochem. Cosmochim. Acta*, v. 38, p. 1007-1022.

PIRONON, J., ROCHDI, A., BARRES, O., BURNEAU, A., LANDAIS, P., PAGEL, M., and POTY, B., 1991, Applications of FT-IR microspectroscopy in the earth sciences. *In* Proceedings of the International Workshop on Fourier transform Spectroscopy, Antwerp, Belgium, p. 281-291.

POHL, W., 1989, Comparative geology of magnesite deposits and occurences: *Monograph Series Mineral Deposits* (P. Moller, ed.), v. 28, p. 1-13.

POHL, W., 1990, Genesis of magnesite deposits - models and trends: *Geologische Rundschau*, v. 79, p. 291-299.

POHL, W. and SIEGL,W., 1986, Sediment-hosted magnesite deposits. *In* K.H. Wolf, ed., Handbook of strata-bound and stratiform ore deposits. Elsevier, Amsterdam, v. 14, p. 223-310.

PREINFALK, C., LUGLI, S., and MORTEANI, G., 1993, The magnesite in the Upper Triasic Burano Evaporitic Formation of central Italy: a contribution to the controversy on sparry magnesite genesis. Terra Abstracts. EUG VII Strasbourg, France, p. 345-346.

QIUSHENG, Z., 1988, Early Proterozoic tectonic styles and associated mineral deposits of the north China Platform: *Precambrian Research*, v. 39, p. 1-29.

QUEMENEUR, J.M., 1974, Les gisements de magnesite du Pays Basque: cadre géologique et sédimentologique; genèse de la magnésite en milieu sédimentaire. Thèse de doctorat présentée à l'Université de Paris VI. 265 p. (unpublished).

SA, J.M., 1991, Evolution geodynamique de la ceinture protérozoique d'Orós. Nord-Est du Brèsil. Thèse de doctorat de l'Université de Nancy I, 117 p.

SCHUL, O. and VAVTA, R.F., 1989, Genetic fabric interpretation of the magnesite deposit of Weißenstein (Hochfilzen. Tyrol): *Monograph Series Mineral Deposits*, v. 28, p. 115-134.

SERDYUCHENKO, D.P., 1975, Some Precambrian scapolite-bearing rocks evolved from evaporites: *Lithos*, v. 8, p. 1-7.

SHAW, D.M., 1960, The geochemistry of scapolite. Parts 1 and 2:

Journal of Petrology, v. 1, p. 218 -285.

SIAL, A.N., FERREIRA, V.P., ALMEIDA, A.R., ROMANO, A.W., PARENTE, C.V., COSTA, M.L., and SANTOS, V.H., 2000, Carbon isotope fluctuations in Precambrian carbonate sequences of several localities in Brazil: *Anais da Academia Brasileira de Ciências*, v. 72, p. 539-558.

SIEGL, W., 1984, Reflexions on the Origin of Sparry Magnesite Deposits. *In* A. Wauschkuhn, C. Kluth, and R.A. Zimmermann, eds., Syngenesis and Epigenesis in the Formation of Mineral Deposits. Springer-Verlag, Berlin-Heidelberg, p. 177 -182.

SVENNINGSEN, O.M., 1994, Tectonic significance of the meta-evaporitic magnesite and scapolite deposits in the Seve Nappes. Sarek Mts. Swedish Caledonides: *Tectonophysics*, v. 231, p. 33-44.

TLIG. S., 1987, The Sr and rare earth element (REE) behaviour during diagenesis of limestone in various environmental conditions. *In* R.W. Hurst, T.E. Davis, and S.S. Augustithis, eds., The pratical applications of trace elements and isotopes to environmental biochemistry and mineral resources evaluation. Theophrastus Publications, S.A., p. 103-147.

TUFAR, W., GIEB, J., SCHMIDT, R.S., MÖLLER, P., PÖHL, W., HIEDLER, H., and OLSACHER, A., 1989, Formation of magnesite in the Radenthein (Carinthia/Austria) type locality: *Monograph Series Mineral Deposits*, v. 28, p. 135-171.

VALDIYA, K.S., 1968, Origin of the magnesite deposits of Southern Pithoragarh. Kumaun Himalaya, India: *Economic Geology*, v. 63, p. 924-934.

VANKO, D.A. and BISCHOP, F.C., 1982, Occurence and origin of marialitic scapolite in the Humboldt lopolith. N.W. Nevada: *Contrib. Mineralogy, Petrology*, v. 81, p. 277-289.

VAN SCHMUS, W.R., BRITO NEVES, B.B., HACKSPACHER, P., and BABINSKI, M., 1995, U/Pb and Sm/Nd geochronologic studies of the eastern Borborema Province. Northeastern Brazil: initial conclusions: *J. South American Earth Sciences*, v. 8, p. 267-288.

VELASCO, F., PESQUERA, A., and OLMEDO, F., 1987, A contribution to the ore genesis of the magnesite deposit of Eugui. Navarra (Spain): *Mineralium Deposita*, v. 22, p. 33-41.

VEIZER, J., CLAYTON, R.N., HINTON, R.W., BRUNN, V.V., MASON, T.R., BUCK, S.G., and HOEFS, J., 1990, Geochemistry of Precambrian carbonates: 3-shelf seas and non-marine environments of the Archean: *Geochim. Cosmochim. Acta*, v. 54, p. 2717-2729.

VEIZER, J., CLAYTON, R.N., and HINTON, R.W., 1992, Geochemistry of Precambrian carbonates: IV. Early Paleoproterozoic (2.25±0.25 Ga) seawater: *Geochim. Cosmochim. Acta*, v. 56, p. 875-885.

VON DER BORG, C.G. , 1965, The distribution and preliminary geochemistry of modern carbonate sediments of the Coorong Area, South Australia: *Geoch. Cosmoch. Acta*, v. 29, p. 781-799.

VON DER BORG, C.G., 1976, Stratigraphy and formation of Holocene dolomitic carbonate deposits of the Coorong Area, south Australia: *Journal of Sedimentary Petrology*, v. 46, p. 956-966.